

STUDY ON THE EARLY STREAMER EMISSION MECHANISMS  
AIDED BY LASER RADIATION IONIZATION PROCESS

(KAJIAN TERHADAP MEKANISMA EMISI PENJURUS AWAL  
YANG DIBANTU DENGAN PROSES PENGIONAN RADIASI  
LASER)

PROF. DR. HUSSEIN BIN AHMAD

RESEARCH VOTE NO:  
74276

Department of Electrical Power Engineering  
Faculty of Electrical Engineering  
Universiti Teknologi Malaysia

## ACKNOWLEDGEMENTS

Praise be to ALLAH, the Lord of the Worlds, and peace and blessing be upon the most noble of the Prophets and Messengers, our Prophet Muhammad SAW, and upon all his families and companions.

I would like to thank to all technical staff in Institut Voltan dan Arus Tinggi (IVAT) at Faculty of Electrical Engineering UTM for their assistance and providing facilities to carry out this work.

Eventually the author is indebted to the staff of Research Management Centre, University Teknologi Malaysia and MOSTI (Ministry of Science, Technology and Innovation) of Malaysia that providing the financial support and cooperation for this research work.

## ABSTRACT

Lightning, considered as a spectacular meteorological phenomenon, is one of the most fascinating events in the world. The preliminary scientific and systematic understanding of lightning phenomenon was first constituted by Benjamin Franklin in 1752 that used a kite in order to verify that lightning is really a stream of electrified air. Interestingly when Benjamin Franklin experimented with the electric kite, there were no very tall structures and high rise buildings like we observed today. However till today over more than 200 years the Benjamin's lightning rod is still the most internationally accepted LAT. Many standards of LPSs have been published. Among which are the following standards: BS 6651 (British), NFPA 780 (American), IEC 61024-1-2. These standards discuss and outline all important aspect of LPSs including design and methods for installing lightning terminal, bonding, and zone of protection calculation. However, these standards utilize Franklin rod concept for their lightning terminals. Even though these standards give some guidance and recommendations for installation of lightning protection, the standard can not assure the systems can provide 100% protection because there are evidences showing these systems can experience malfunctioning. A LAT tip can be damage by harsh environmental condition for instance due to acid rain that will affect on corona emission pattern. Corona developed on a tip of LAT have affect on the performance of the LAT. To study corona on the damage conventional lightning air terminal a new testing set-up was introduced. This testing set-up was completed with humidifier system, temperature control room and adjustable in high of cloud simulation disk. Indigenous Electric Field Mill system was developed. It was completed with a terminal to ADC before a PC (for display, analysis, and data collecting), a personal warning system, and an infra red unit (to initiate laser unit in LPS). The corona emission patterns on the damage convention LATs were acquired from the corona study. Further an empirical model by using dimension analysis was acquired. From this series of works an intensive reviewed published literature on lightning air terminal and lightning protection system was accomplished. A new model of LAT which is still conventional completed with free charge generator and laser unit was introduced.

## ABSTRAK

Kilat, sebagai sebuah kejadian meteorologi yang menakjubkan, adalah satu dari kejadian paling menarik di dunia. Permulaan pemahaman secara saintifik dan sistematik yang berkenaan dengan kilat dilakukan oleh Benjamin Franklin pada tahun 1752, yang menggunakan sebuah layang-layang untuk mengetahui dengan benar apakah kilat merupakan strom dari udara yang mengandung energi listrik. Apa yang menarik pada percobaan Benjamin Franklin adalah pada saat itu belum adanya struktur-struktur dan bangunan yang sangat tinggi sebagaimana saat ini. Bagaimanapun sampai pada saat ini setelah lebih dari 200 tahun terminal udara kilat yang diperkenalkan oleh Benjamin masih menjadi terminal udara kilat yang paling diterima. Banyak standar-standar sistem perlindungan kilat yang telah dipublikasikan. Diantaranya adalah: BS 6651 (British), NFPA 780 (America), IEC 61024-1-2. Standar-standar ini mendiskusikan dan mengemukakan semua aspek-aspek penting dari sistem perlindungan kilat termasuk perancangan dan kaedah bagi pemasangan terminal udara kilat, bonding, dan perhitungan zona perlindungan. Standar-standar ini menggunakan konsep batang udara Franklin sebagai terminal udara kilat. Walaupun standar-standar ini memberikan sejumlah petunjuk dan rekomendasi untuk pemasangan sistem perlindungan kilat, standar ini tidak dapat menjamin 100% perlindungan, ditemukan banyak bukti bahwa sistem ini mengalami kegagalan. Bagian puncak dari suatu terminal udara kilat boleh menjadi rosak kerana kondisi alam yang buruk sebagai contoh kerana hujan asam, hal ini akan mempengaruhi bentuk emisi korona. Pembentukan korona pada puncak terminal udara boleh berpengaruh kepada performanya kerja dari terminal udara kilat. Untuk mengetahui bentuk korona pada terminal udara kilat yang rosak sebuah setup baru telah diperkenalkan. Setup pengujian ini dilengkapi dengan sistem pelembab udara, pengatur suhu udara ruangan, dan simulasi awan yang ketinggiannya dapat disesuaikan. Sebuah sistem pengukur medan elektrik telah dikembangkan. Ianya dilengkapi dengan sebuah terminal sebagai keluaran kepada perubah analog kepada digital (ADC) sebelum masuk kepada komputer (untuk paparan, analisa, dan pengambilan data), sebuah sistem peringatan dini, dan sebuah unit infra-red (untuk mengaktifkan unit laser pada sistem perlindungan kilat). Bentuk emisi korona pada terminal udara kilat yang rosak didapat dari kajian korona ini. Selanjutnya sebuah bentuk empirik dengan menggunakan analisa dimensi diperoleh. Dari kajian ini suatu intensif review dari literatur yang telah diterbitkan berkenaan dengan terminal udara kilat dan sistem perlindungan kilat telah dilakukan. Sebuah reka bentuk baru daripada terminal udara kilat telah dibuat dengan mengaplikasikan pembangkitan muatan bebas dan unit laser.

## TABLE OF CONTENTS

<b>CHAPTER</b>	<b>CONTENTS</b>	<b>PAGE</b>
	<b>TITLE</b>	i
	<b>ACKNOWLEDGEMENTS</b>	ii
	<b>ABSTRACT</b>	iii
	<b>ABSTRAK</b>	iv
	<b>TABLE OF CONTENTS</b>	v
	<b>LIST OF FIGURES</b>	viii
	<b>LIST OF TABLES</b>	xi
	<b>LIST OF SYMBOLS</b>	xii
	<b>LIST OF APPENDICES</b>	xiv
<b>1</b>	<b>INTRODUCTION</b>	<b>1</b>
	1.1 Background	1
	1.2 Lightning Protection System Standards	4
	1.3 The Epilogue Of LAT	5
	1.4 Laser-Triggered Discharges	9
	1.5 Direction of the Research and Objectives	12
	1.6 Scope of the Research	12
	1.7 Original Contributions	13
	1.8 Structure of the thesis	13
<b>2</b>	<b>CORONA DISCHARGE OF CONVENTIONAL LIGHTNING</b>	
	<b>AIR TERMINALS</b>	<b>14</b>
	2.1 Introduction	14
	2.2 A New Experimental Set-up	15

2.3	Experimental Procedures	18
2.4	Results and discussion	19
2.5	Dimensional analysis	21
2.6	Conclusion	24
<b>3</b>	<b>DEVELOPMENT OF INDIGENOUS ELECTRIC FIELD MILL FOR EARLY WARNING AND TRIGGERING LASER SYSTEM</b>	<b>28</b>
3.1	Introduction	28
3.2	Thunderstorm Formation And It Electrification Process	31
3.3	Electric Field Strength	33
3.4	Indigenous Rotating -vane Electric Field Mill	33
3.4.1	General Principle of the REFM	34
3.4.2	Developed REFM	34
3.4.3	Signal Processing	35
3.4.3.1	Amplification unit	36
3.4.3.2	Filtering, Conversion, and Conditiner Unit	38
3.4.4	Microcontroller Unit	41
3.4.5	Relay Board Unit	43
3.4.6	Integrated Unit	45
3.5	The REFM Calibration	46
3.5.1	Methodology	46
3.5.2	Calibration Results and Discussion	48
3.6	Early Warning System and Laser Triggering System	55
3.6.1	Early Warning System	56
3.6.2	Laser triggering system	56
3.7	A new concept of lightning protection system for strategic areas	60
3.7.1	Simulation of the new concept	61
3.7.2	Computer Measuring System	63

<b>4</b>	<b>DEVELOPMENT A NEW DIRECT STRIKE LIGHTNING AIR TERMINAL USING ELECTROSTATIC GENERATOR CONCEPT</b>	<b>65</b>
4.1	Introduction	65
4.2	Objective	68
4.3	Scope of work	68
4.4	Research Methodology	69
4.4.1	Conceptual design	69
4.4.2	Computer modelling	74
4.4.3	Development the Prototype	76
4.5	Experimental Setup	78
4.6	Results and Discussion	81
4.7	Conclusions	83
<b>5</b>	<b>GENERAL CONCLUSIONS AND FUTURE WORKS</b>	<b>84</b>
5.1	General Conclusions	84
5.2	Future Works	85
	<b>REFERENCES</b>	<b>86</b>
	<b>APPENDICES A – F</b>	

## LIST OF FIGURES

FIGURE NO.	TITLE	PAGE
Figure 1. 1	The situation in Pasir Gudang, Johor, Malaysia.	2
Figure 1. 2	Building structure equipped with a monopole at the roof top at the central and extreme edge of the building still being damaged by lightning stroke in spite of LAT installed.	4
Figure 1. 3	Rocket Triggered Lightning (Rakov 2006)	5
Figure 2. 1	The novel air humidifier testing system, (a) Schematic diagram of the controlled room, and (b) The experimental set-up of corona emission.	17
Figure 2. 2	Pictorial view of test set-up, (a) Front, (b) Right	17
Figure 2. 3	Pictorial view of leakage current sensor box	18
Figure 2. 4	Various types of LAT	18
Figure 2. 5	Corona discharge on LAT tips, (a) standard, (b) concave, (d) flat, and (e) conical.	20
Figure 2. 6	The area of LAT that produce corona discharge current.	20
Figure 2. 7	Electric field versus corona discharge current of Standard LAT.	24
Figure 2. 8	Electric field versus corona discharge current of Concave LAT.	24
Figure 2. 9	Electric field versus corona discharge current of Flat LAT.	25
Figure 2.10	Electric field versus corona discharge current of Conical LAT.	25
Figure 2.11	Obtained results of 6-kV/cm electric field and the corona discharge current.	26
Figure 3.1	Cloud's names are based on the shape and the altitude of the clouds [48].	31
Figure 3.2	Rotating-vane type EFM	35



Figure 3.3	The signal amplification unit, (a) Schematic diagram, (b) Amplifier board, and (c) Aluminium box.	37
Figure 3.4	The output of signal amplification unit	38
Figure 3.5	Simplified schematic of AD536	39
Figure 3.6	The filter, converter, and conditioner unit, (a) schematic diagram and (b) electronic circuit	40
Figure 3.7	The sample of signal output from	41
Figure 3.8	The microcontroller unit integrated with the emulator circuit, (a) Schematic diagram and (b) Circuit board	43
Figure 3.9	The relay board unit, (a) Schematic diagram and (b) Electronic circuit	44
Figure 3.10	The integrated unit, (a) top view, (b) front view, and (c) back view	46
Figure 3.11	The general of REFM calibration setup	47
Figure 3.12	The REFM calibration setup	48
Figure 3.13	The results of online calibration measurement according to the distance of the cloud simulation to the REFM, (a) 30-cm, (b) 48-cm, and (c) 70-cm.	50
Figure 3.14	Simultaneous measurement results	51
Figure 3.15	Mathematical equation models of simultaneous measurement results: (a) Linear, (b) Exponential, and (c) Power.	55
Figure 3.16	The mock-up of early warning system, (a) Schematic diagram and (b) The alarm unit with a cable length to the integrated unit	56
Figure 3.17	The infra-red remote control transmitter, (a) Transmitter schematic diagram and (b) remote infra red unit	58
Figure 3.18	The infra-red remote control receiver and the Laser system, (a) Receiver schematic diagram, (b) Laser triggering system 20.0-mW, and (c) Laser triggering system 1.0-mW	59
Figure 3.19	The diagram of the novel concept of LAT for strategic areas	60
Figure 3.20	The simulation, (a) Block diagram and (b) Front panel	62
Figure 3.21	Front Panel of VMI of the EWarS&Laser version 1.05	64
Figure 4.1	Malaysia location in the globe [2].	65

Figure 4. 2	Lightning Map the black area in Central Africa is where the greatest lightning activity occurs. Reds, oranges and yellows are areas of high activity while areas in white or blue have low activity [3].	66
Figure 4. 3	Process flow of LAT prototype development.	68
Figure 4.4	Varley machine [5].	70
Figure 4. 5	Schematic diagram of electrostatic generator model.	71
Figure 4. 6	Electrostatic generator model.	71
Figure 4. 7	Numerous outputs of electrostatic generator model.	73
Figure 4. 8	Computer model of DS LAT, (a) Full model and (b) Section view of the new DS LAT.	75
Figure 4. 9	Diagram of electrostatic generator applied on DS LAT.	76
Figure 4. 10	New direct strike lightning air terminal, (a) first prototype, and (b) second prototype.	77
Figure 4. 11	General setup of the competitive testing.	78
Figure 4. 12	Testing setup for First prototype, showing the distance of the competitive test.	79
Figure 4. 13	Testing setup for Second prototype, showing the distance of the competitive test.	79
Figure 4. 14	Tested LAT samples positions	80
Figure 4. 15	First prototype testing results.	81
Figure 4. 16	Second prototype testing results.	82
Figure 4. 17	A result of lightning impulse discharge of the competitive test for the first prototype where the upward streamer was also developed on the tips of the conventional LAT.	82
Figure 4. 18	A result of lightning impulse discharge of the competitive test for the second prototype.	82

**LIST OF TABLES**

<b>TABLE NO.</b>	<b>TITLE</b>	<b>PAGE</b>
Table 2. 1	Tips' Profile Of LAT	21
Table 3. 1	The constant calculation results and correlation coefficient	53
Table 3. 2	The simulation block components	61

## LIST OF SYMBOLS

SYMBOL	MEANING
$A$	area produce corona
$\text{mm}^2$	millimetre square
$I_{cd}$	corona discharge current
$\epsilon$	permittivity
$T$	time
$d$	distance
$V$	voltage
$L$	length
$M$	mass
$Q$	charge
$D_c$	dimensionless constant
$\text{mA}$	milliampere
$E$	electric field
$\text{kV}$	kilovolt
$\text{cm}$	centimetre
$\text{m}^2$	metre square
$V_{IN}$	input voltage
$I$	current
$R$	resistor
$C$	capacitor
$C_{AV}$	external connected capacitor
$\text{ms}$	millisecond
$I_{OUT}$	output current
$V_{OUT}$	output voltage
$W$	watt
$V_{in-trans}$	input voltage transformer

$V_{out-int}$	output voltage integrated circuit
mV	millivolt
$V_{efm}$	electric field mill voltage
$\alpha$	constant
$\beta$	constant
$\hat{y}$	dependent/response variable.
$\hat{\alpha}$	intercept coefficient.
$\hat{\beta}$	independent regression coefficient.
$x$	independent/regressor variable.
$r$	correlation coefficient
$R^2$	multiple correlation coefficient
h	height
mW	milliwatt
MV	megavolt
$\mu$ s	microsecond
m	metre
mp	megapixel

**LIST OF APPENDICES**

<b>APPENDIX</b>	<b>TITLE</b>	<b>PAGE</b>
A	BLOK DIAGRAM OF VIRTUAL MEASUREMENT INSTRUMENT	94
B	DETAIL DESIGN OF NEW LIGHTNING AIR TERMINAL	106
C	PROTOTYPE TESTING RESULTS	131
D	DATA SHEETS	134
E	AWARDS	146
F	PUBLICATIONS	150

## **CHAPTER 1**

### **INTRODUCTION**

#### **1.1 Background**

Lightning, considered as a spectacular meteorological phenomenon, is one of the most fascinating events in the world. The preliminary scientific and systematic understanding of lightning phenomenon was first constituted by Benjamin Franklin in 1752 that used a kite in order to verify that lightning is really a stream of electrified air. Interestingly when Benjamin Franklin experimented with the electric kite, there were no very tall structures and high rise buildings like we observed today. However till today over more than 200 years the Benjamin's lightning rod is still the most internationally accepted Lightning Air Terminal (LAT).

Lightning current in a lightning stroke if penetrated in a human body can injure any internal organs, cease heart function, and damage the nerve system. According to storm data recorded by the National Weather Service, in US between 1959 and 1994 there were 3,239 deaths and 9,818 others injured as a result of lightning strokes. Another storm data from National Lightning Safety Institute (NLSI) illustrated that from 1990 to 2003 there were 756 people killed due to lightning strokes. Industrial structures like petrochemical complexes, nuclear power plants, rocket-launching pad, and others may turn out to be extremely hazardous when they were struck by lightning [1].

The Indonesian oil refinery owned by Pertamina in Cilacap, on the southern coast of Java, blown up in October 1995 as a result of lightning stroke. The refinery

tank made from 10-cm plate exploded. In just few minutes the burst from the first tank was followed by six other neighbouring tanks. Even though there was no serious casualty, evacuation has to be conducted for thousands of Cilacap residents and about 400 Pertamina employees. These tanks have capacity to supply about 34% of Indonesia internal oil consumption for a period of 18 months. As the result of the that incident Indonesian government had to import oil, petrol, kerosene, and diesel at the cost worth approximately USD 430,000.00 daily for the Java island consumption alone. Pertamina was able to restart its own production only after about 2 (two) years after the incident happened [2].

Almost similar with Pertamina incident, recently on April 28, 2006, at around 06.00-pm, the Malaysia government's petroleum company, Petronas, oil tanks blown up as result of lightning stroke in Pasir Gudang, Johor. In that incident not less than 8 (eight) tanks were fired up. The fire reached up about 20 (twenty) metres height and produced very thick smog which was able to be seen in radii of 6 (six) kilometres from incident location. Figure 1.1 illustrates the situation of location.



Figure 1.1: The situation in Pasir Gudang, Johor, Malaysia.

In 1992, major power system grid in eastern Malaysia was disrupted by lightning stroke that crippled the power system across the nation. The lost of revenue was about RM 220 millions. Meanwhile, in Mexico lightning has caused more than 50% of the total outages in the 115-kV to 400-kV transmission line [3,4].

The most popular major incident due to lightning in aerospace activities occurred during the launching of Apollo 12 mission. The lightning had caused temporary malfunction of vital electronic instruments in the spacecraft. This became



the reason for NASA to pursue lightning research. Lightning strikes at the vicinity of aircraft often originate from the body of craft itself. The flash started with the inception of a leader, propagating in both directions away from the craft. These are called triggered lightning flashes [5,6].

Besides aircraft, other man-made systems are also constantly under the threat of the hazards of lightning strokes due to direct or indirect flashes. From a survey [34] it was found out that from 1995 to 2000 almost 50% of the telecommunication utilities suffered damages to equipment due to lightning related causes. These threats cause system downtime, loss of production and revenue plus increase in customer frustration and loss in market competitiveness. Lightning protection system (LPS) vendors offered many solutions to mitigate damages to man-made system due to lightning. However, so far there are still problems of protection of terrestrial objects against lightning. Appolonov, V.V. et al., [1] stated that the existing LPSs being used currently were not always in a position to ensure the desired level of efficiency. It can be consolidated from the study conducted by Norfizah, O., and Zafirah, A., [34] saw that even conventional air terminals suffered with the problem of inefficiency in capturing lightning downwards leader and consequently being translated into structures frontal and corners damages as shown in Fig. 1.2.

The development and research on technologies to control or even to prevent lightning strokes still continues until the present period. As most people use many electrical devices which are sensitive to electrical system disturbances, in their daily activities. The existence and development of a reliable lightning protection system is therefore, very essential [7].

Generally lightning protection can be categorised into two different types. One is by collecting the lightning strokes, using the conventional LAT (Franklin rod) and several types of Early Steamer Emission (ESE) LAT. The latter is an LAT that generally comprises a special unit attached near the top of the terminal or special shaped LAT. According to the vendors, it is theoretically designed to develop an upward propagating streamer faster than the one generated from a conventional LAT. They claimed that with ESE, the upward streamer launched can reach up to  $1 \times 10^6$  m/sec whereas the acceptable streamer speed is in the order of  $10^5$  m/sec.



Figure 1. 2: Building structure equipped with a monopole at the roof top at the central and extreme edge of the building still being damaged by lightning stroke in spite of LAT installed.

## 1.2 Lightning Protection System Standards

Many standards of LPS have been published. Among which are the BS 6651 (British), NFPA 780 (American), and IEC 61024-1-2 standards. These standards discuss and outline all important aspect of LPSs including design and methods for installing LAT, bonding, and zone of protection calculation. However, these standards utilize Franklin rod concept for their LAT. Even though these standards give some guidance and recommendations for installation of lightning protection, they can not assure the systems can provide 100% protection because there are evidences showing these systems can experience malfunctioning. Figure 1.2 shows that the lightning struck the building edge, though of the Franklin rod is installed.

The standard advocate the use of standard LAT is due to the principle of operation of LAT is based on sacrificial point of stroke. However Figure 1.2 shows the failure of LAT to perform as a point most likely to be struck by lightning leaders. The interesting part that has been shown in [8], concern the mechanics and dynamics of lightning leader attachment to the ground and associated structure as in Figure 1.3.

Figure 1.3 shows a lightning stroke initiated in 1999 from the underground launcher at the centre of 70 x 70 m<sup>2</sup> buried metallic grid at Camp Blanding Florida. From here what can be said is that a rocket which has a ground wire attached to it is launched upwards after the magnitude of electric field surpassed a threshold value indicative of lightning stroke. If the target is right, and lightning downwards leader is formed and strike the rocket head and flows downward through the wire which is connected to the metallic grid. The attachment points on the ground surface are numerous not a single concentrated point but multiple. Only a fraction is attached to the LAT as indicated with the arrow. However this model is not the perfect model to explain the malfunctioning of LAT. The best method is to capture the actual scenario of lightning leaders' attachment to buildings.



Figure 1.3: Rocket Triggered Lightning (Rakov 2006)

### 1.3 The Epilogue Of LAT

Franklin rod, the oldest LAT proposed by Dr. Benjamin Franklin who first thought that a terminal could silently discharged the electric charge in a thundercloud and thereby prevented lightning. However, in 1755 he inferred that point rods erected on buildings would conduct lightning strokes so that the building should suffer no damage. Since the charge flowing between a LAT and a thunder cloud is much too small to discharge the thundercloud. However not all scientists agreed with Franklin at that time. Some of Franklin's contemporaries believed that having a point atop the rod was either futile or sure to cause problem. One of the most eloquent critics of Franklin was Benjamin Wilson. In his opinion such rod less safe than not pointed rods. Every point solicits lightning stroke and as a result not only contributes to increase in the quantity of every actual discharge, but also frequently occasioning a discharge. Wilson believed using points would cause possibility of lightning attacks than that experienced. Alternately, he proposed the blunt rod system and referred to one installed on the new Eddystone Lighthouse. This new building was not been struck by lightning for about 12 (twelve) years, although, in the past, a difference building in the same location had been set on fire due to a lightning stroke [9].

Wilson was supported by Edward H. De Laval on the issue of the futility of trying to drain a cloud of its charge. De Laval revealed that the quantity of lightning, which could be drawn from large thunderclouds by mean of conductor, was so very small a part of the whole contained in them, that any attempts to exhaust them had to be looked upon as altogether vain [9].

However, after that period new innovations or inventions in conjunction with the LAT shapes and concepts are not found in any published literatures until the early of nineteenth century.

It is Szillard, J.B, who presented his paper to the Academy of Science in Paris, on March 9, 1914, came with new idea concerning of LAT. His idea became a foundation for the use of ionisation method for lightning protection innovation. Later on in 1931, Gustav P. Carpart patented the first ionising LAT. Gustav's son, Alphonse Capart, in 1953, started to improve the device and commercialised his development [10]. The LAT is equipped with ionisation generator supposedly ionise

the air molecules in the immediate vicinity of the LAT continuously, with or without the presence of a storm cell. The ionisation generator is radioactive material. This kind of LAT also referred then as ionising or radioactive LAT.

However, in 1965 the British Standard Committee as described in BS CP 326:1965 rejected the use of radioactive LAT. Afterwards the use of them was banned in many countries due to the possible human exposure to harmful radiation.

For the review, starting in the 1980s, the LATs encompassed with electrical triggering device were introduced. In principle, their purpose is the same as a radioactive source. However, unlike a rod equipped with a radioactive source that causes continuous ionisation in the surrounding air, they give more control over ion production at the tip of the terminal at which the electrically triggered device produces ionisation only during a brief period prior to the lightning stroke. They also avoid the health and environment issues that are associated with radioactive device but the information about the duration and extent of this ionisation could not be found. The manufactures of this terminal claimed that the device can improve the probability of initiating an upward streamer to connect with downward propagating leader of a lightning stroke. It means that the first streamer reaches the thermal stage before others; therefore this terminal is namely as ESE LAT.

It is found that at present there are three methods in producing the electrical triggering for lightning terminal. They are base on geometrical configuration, by using an auxiliary power apparatus, and by means of a piezoelectric device [11,13].

Basically the principle of the geometrical configuration based LAT is to absorb the ambient electrical energy. The energy which is acquired from the electrical field intensity during the approach of a lightning stroke is used to charge a capacitor which is subsequently used to generate sparks discharge to the nearby grounded rod. From published literature, it is found that the energy absorber can be a set of sensor in a sharp form, or a floating semi-spherical dome [33].

The auxiliary power apparatus based LAT uses batteries and photo cells to produce voltage pulse, and a detector that sense the approach of a downward propagating leader. The detector produces an electrical signal proportional either to electric field or rate-of-change of electric field produced by approaching leader [33].

The LAT which incorporated with piezoelectric device was patented by Robert Andre, et al [11]. This lightning conductor pole put on a support fixed by using a ball. Under the action of the wind, the pole moved out of the vertical position

until a shoulder abuts against a flange of the support. With the wind continuing to act on the pole, the latter applied a considerable force on the support. The reaction force or torque was transmitted to the piezoelectric device by using the ball. Even though this type of terminal is now available commercially [12], there are very little published information about performance of the lightning terminal with the piezoelectric device.

Until today, a complete and universally accepted scientific explanation on how ESE LATs work has not yet been established. Particularly on the claim that with ESE, the upward initiated streamer can be launched if the speed that can reach up to  $1 \times 10^6$  m/sec whereas the acceptable streamer speed is in the order of  $10^5$  m/sec. The proponents and opponents of the ESE LATs have different perception regarding the performance of ESE LATs. Van Brunt, R.J., [12] revealed that proponents of the ESE LATs claimed that the lack of credible statistical data on failure of these LATs prove their effectiveness, meanwhile opponents of these LATs argue that a lack of evidence about the improved performance of these terminals over conventional terminals prove their ineffectiveness. In this paper they examined the physical basis for ESE devices and identified areas of controversy and gaps in human knowledge of lightning and lightning protection that need to be considered in assessing ESE devices and in their future development.

Hartono and Robiah [13] published a report on the study of some buildings situated in Kuala Lumpur and Shah Alam, Malaysia installed with ESE LATs. By using lightning interception prediction method they acquired the pre-strike and post-strike photographs of the affected building.

In United State the issue of ESE brought the proponents and the opponents of ESE to court. In 1998, the NFPA agreed to re-open the study to determine whether any new information behind the claims made by ESE vendors and continued by the NFPA upheld their 1995 rejection of the proposed NFPA 781 standard, in 2000. The ESE vendors then sued those who claimed that the ESE vendors are making false claiming that the ESE lightning rods have large protection radii.

On October 7, 2005, the United States District Court of Arizona issued an injunction which prohibits the vendors of ESE from providing range of their gadgets claiming to be better than that of a Franklin rod. The order also dismissed all claims of the vendors of ESE gadgets and granted the counterclaims of all dependents.

Another type of LAT which is categorised as preventive method of lightning protection and commonly known as Charge Transfer System (CTS) LAT. The concept of LPS based on CTS started in 1754 when Czech scientist, Prokop Divish, proposed the idea of using multi point discharge to neutralise cloud charge in order to prevent lightning strokes. Since then this concept of LPS has become a controversy among lightning scientists till today. Interestingly, J.M. Cage, a southern Californian who was an oil-field worker, succeeded in patenting a multipoint discharge system to prevent lightning stroke in 1930. The systematic commercialization of the CTS, however, started in 1971. A prototype was developed and later marketed by Roy Carpenter, Jr. Description on the principle of operation and physical theories behind the CTS are found in some published papers [10,14,15,16,17,18]. Although the manufacturers of CTS proclaimed that the CTS are developed on the basis of physical theories; however, the laboratory tests and some field observations have proved that CTS cannot fully prevent lightning strokes [19].

In the beginning Franklin proposed the application of a sharp rod for LAT but some scientists like Wilson and De Laval proposed the use of a blunt rod, instead of a sharp rod, for the prevention of building from the lightning strikes. In another report from Moore, C.B., et al [20] suggested a moderately blunt rod of a specific ratio between the height to the tip radius of curvature is a better lightning receptor than sharper rod or a very blunt one. This findings is in agreement with the results obtained by Ong L. M., et al [21] that proved the effectiveness of blunt rod compared to the other 5 (five) different LATs' tip configuration.

#### **1.4 Laser-Triggered Discharges**

Einstein, in 1917, introduced the concept of stimulated emission. After forty years later, Schawlow and Townes gave the idea about light amplification of stimulated emission radiation (laser). In 1960, Maiman succeeded to demonstrate the first laser produced from ruby rod in laboratory of Hughes Aircraft Company, California. It was a pulse laser, 694.3-nm, namely ruby laser. Koopman and Wilkerson [22] conducted an experiment in which a long electrical spark discharges

was directed through air along predetermined paths defined by a concentrated laser beam. He founded that the average E field required to obtain a discharge between electrodes was reduced from 7.3-kV/cm to 5.5-kV/cm with the laser powers employed.

In 1974, Ball, L.M. [23] suggested a possibility of the application of a laser lightning rod. Schubert, Jr., and Lippert [24] presented an experimental model of the laser lightning rod with pulse laser.

Laser guided discharge is very different from those of unguided discharges. Laser could reduce the flashover voltage of a gap. This phenomenon is closely related to the trigger effect of laser. When a high power laser beam is focused in air, a high degree of ionisation could be produced in brilliant bead at the plasma focus [25]. This is a well-known phenomenon called optical breakdown. If the power of the laser is high enough a chain of air breakdown plasmas are produced along the laser beam. The stepped progression of the negative leader along laser produced plasmas required only a small electric field. [25]. Bruno, et al [26] described that further simplification could be brought about by using as little laser energy as possible while maintaining a triggering ability, so that the plasma heating is kept to a minimum.

The experimental results indicated that negative electrical discharges were appropriate to be guided by the laser-produced by the laser produced-plasmas. Floating particles had an ability to guide electrical discharges, especially in the case of a negative polarity [27]. Comtois, D., et al [28] reported that laser pulse could initiate a corona at the tip of the positive rod and instantaneously trigger leader propagation, at a voltage that could be 30% lower than the normal minimum inception voltage of the first corona. This technique is potentially very interesting because the natural breakdown voltage could be significantly reduced, the discharge could be precisely located in space and time, and it could be initiated from a distance [26].

The mechanism of the guiding ability of the laser could be explained by the behaviour of the plasma as a conductor [29]. The laser ability to trigger and guide discharge is due to the laser-produced plasma distort the ambient electric field. Laser could produce multi-photon ionisation [10].

The laser can guide a lightning leader that is propagating towards the earth. It can function as a conductor as if coming from the cloud to the ground and it will



draw the leader to terminate at the LPS. Triggered lightning stroke coupled with the aid of laser were successfully conducted in one of the field experiment near the Sea of Japan. It was found that timing was critical to successfully drawing the lightning strokes in that system [30].

By using laser, the lightning strokes instead of travelling in a zigzag motion it can travel along the laser beam path and hit the ground at a desired spot. One experiment in conjunction with the laser trigger experiment was conducted by Ahmad, H. B., et al [31]. They carried out a set of lightning flashover test in a competitive mode between the laser triggered LAT and non-triggered LAT which involved the use of a 2.0-MV Marx impulse generator. It was reported that the laser triggered LAT has better performance in intercepting the discharges than the non-triggered LAT. It was assumed that the lightning discharge channel developed guided towards the LAT along with the plasma channel formed as a result of the laser-induced breakdown of the atmosphere [1].

Several studies, in the laboratory and field, had shown that the laser triggered lightning technique can be effective in initiating and controlling the path of an electrical discharge in long air gaps. A LP system utilizing intense laser beams to guide a leader discharge has great potentiality to become a promising appropriate technology of LPS in the future.

Ahmad, H.B., et al [31], found that even by using a small laser system, the conventional LAT equipped with laser system is more prone to lightning strike than non-equipped LAT. Thus by using a laser aided system the striking distance of LAT can be increased. This is analogous to having a long monopole for LP. The effective application of this version of Franklin LAT is one of the reasons for the reported low incidence of damages due to direct lightning strokes to buildings in Japan [32].

From the above overview it can be concluded that in any mode of LATs there bound to have merits and demerits. In this respect, concerning the LATs, there are two schools of taught. Actually, the proponents of the conventional method of LPS have lost the zeal and enthusiasm to improve on the 200 years old method of LPS because it is protected by the standard. On the other hand, the proponent of unconventional LPS which has been rejected by the United States District Court of Arizona on the October 7, 2005 and ESE vendors are not allow to claim their products are better than the Franklin Rod. This fact has motivated them to innovate their existing LPS technology. This research project is about developing a Direct

Strike Air Terminal which is better than the 200-year old method of LPS founded by Benjamin Franklin.

### **1.5 Direction of the Research and Objectives**

The study is to acquire a better understanding of lightning air terminal characteristics under the presence of high voltages and high currents. This research is purposed;

- 1) To review and discuss published studies on lightning in order to acquire a better understanding on the principle of the lightning air terminal performance and the lightning streamer attaching process.
- 2) To develop a new lightning terminal encompassed with light amplification by stimulation of emission radiation (LASER).
- 3) To design, construct, and improve the laboratory test set-up for studying pre-discharge activities on LAT.
- 4) To contribute to a better understanding of lightning streamer attachment process under the presence of ionisation of air phenomenon.
- 5) To qualitatively study the effect of LASER and wind on the performance of the new lightning air terminal by carrying out rigorous in-laboratory testing.
- 6) To study the characteristic of the lightning air terminal under simulated laboratory condition.

### **1.6 Scope of the Research**

The scopes of this research are as follows;

- 1) Making a literature study focusing on both the conventional and non-conventional methods of the lightning protection system.

- 2) Designing a lightning air terminal which has a unique feature with the ability to produce corona at the terminal itself.
- 3) Developing an electric field measuring instrument with a computer aided monitoring systems to record and triggers the LASER systems.

## **1.7 Original Contributions**

- 1) An intensive reviewing published literature on lightning air terminal and lightning protection system for conventional and unconventional method of LPS.
- 2) Introduction of a new lightning air terminal which incorporates an innovative technique to enhance the electrical stress at the tip of LAT by using wind-powered rotating mechanism while still maintaining the system categorically conventional.
- 3) Developing a closed-loop mathematical equation to explain the pre-discharge streamers of energized different tip topology lightning air terminal.

## **1.8 Structure of the thesis**

The contents of thesis is planned to be present in five chapters. Chapter 1 presents the background of the research and objective of the study. Chapter 2 describes the developing a close-loop mathematical equation to explain the pre-discharge streamers of energized different tip topology lightning air terminal. Chapter 3 describes the development of Indigenous Electric Field Mill for Early Warning System and Triggering LASER. Chapter 4 present the development of direct strike LAT for strategic area. Chapter 5 presents the general conclusion of this study. And the last Chapter 6 presents the recommendations and future works.

## **CHAPTER 2**

### **CORONA DISCHARGE OF CONVENTIONAL LIGHTNING AIR TERMINALS**

#### **2.1 Introduction**

The corona discharge mechanism under a static electric field is one of the parameters to assess lightning air terminals (LATs) performance. The static electric field strength build-up between the thunder cloud base and the ground passes the minimum value of the dielectric field strength of air causes the propagation of downwards leaders from the cloud base towards the ground initiated the occurrence of in-cloud corona activities.

Moore et al., [20] have conducted experiments to study the comparative competitiveness of a sharp and blunt Franklin air terminal. They found that the blunt rod attracts more lightning leaders attachment than its counterpart. The reason for this to happen is due to the amount of pre-stroke space charge accumulation around the LAT to enhance its ability to initiate and sustain an upward leader [35].

In this connection, a study of corona discharge from two types of LATs, e.g. Franklin rod and ellipsoidal LAT was carried out by Alessandro [36] for quantifying corona discharge phenomenon on the rods' tip under controlled conditions. However, there are others who have conducted experimental studies of LAT performance under uncontrolled condition [37-43].

Interestingly a series of test was conducted by Ong et al., to observe the performance of conventional LATs that have been damaged due to the acid rain

effect [44]. They found that the blunt LAT has better performance to attract lightning downward leader than the others because the blunt LAT does not produce corona discharge as others do. Conclusions were drawn from the results obtained through testing to determine the critical breakdown voltage of different LAT tip configuration.

Whereas this chapter describes an improved method to assess the LAT performance based on corona current measurement technique. However the testing encountered with a problem to continuously maintain corona discharge at LAT's tip for the prescript time. This is due to dependency of corona discharge on humidity level of air. The pre-breakdown streamer heat-up the air surrounding the LAT's tip region thus humidity decreases. This in turn increases the air dielectric breakdown strength and as a result inhibits development of streamers at the LAT's tip.

To overcome this restriction an experimental set-up furnished with an air controller system is required. Hence, a new experimental set-up which is developed in the Institut Voltan dan Arus Tinggi (IVAT), Universiti Teknologi Malaysia, Johor, Malaysia to study corona pre-discharge phenomenon. In line with this, the corona discharge on the different LAT tip configuration were observed.

This chapter describes also in details the development of a closed loop mathematical model based on the study of corona discharges on the various electrodes, in the effort to improve the analysis of the performance of those electrodes under the high voltage DC stresses.

## **2.2 A New Experimental Set-up**

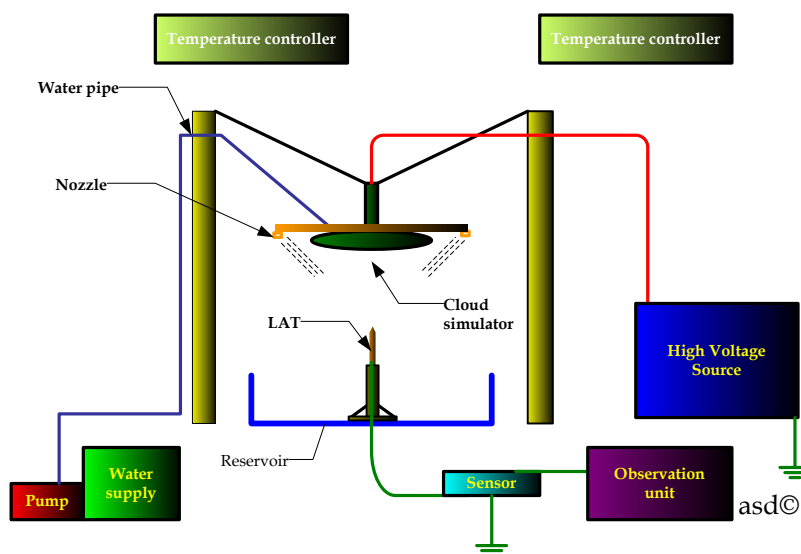
The schematic diagram of the novel experimental set-up which is able to continuously creating corona emission is shown in Figure 2.1 (a). Briefly the set-up consists of an oval shape aluminium high voltage electrode (HVE) which is attached to two plastic-cable supported by a two-pulley-system (TPS), each on both sides. The TPS facilitates clearance variation to enlarge or narrow the air-gap distance between HVE and LAT. While nozzle-type sprinkler along with an electrical pump which is immersed in a tank filled with common tap water, helps to humidify the air.

Figure 2. 1 (b) shows the set-up with a system to capture corona emission activities and leakage current signature capturing system.

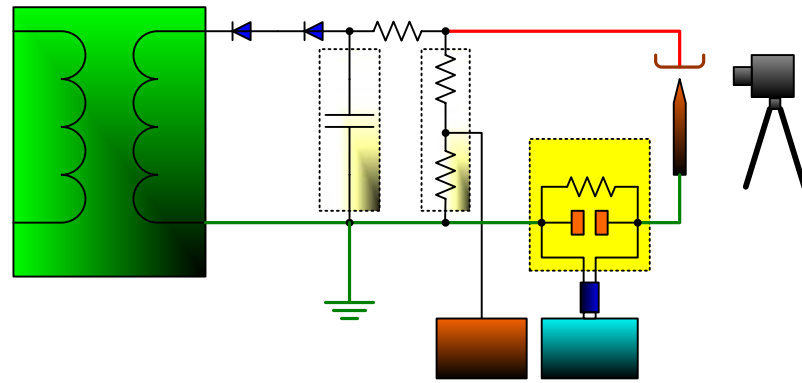
To feed the HVE a HV generator system is used which is basically consists of 230V/100-kV, 5-kVA transformer and a rectifier circuit for high voltage DC generation by means of two 140-kV, 8-kW rectifier diodes and a 25000-pF smoothing capacitor.

The observations of the corona emission current were conducted with the attachment of LATs under test to the experimental rig grounding system via a 1.2-k $\Omega$  resistor. Therefore for 1-V measured across the resistor corresponds to 0.833-mA of corona emission current. For surge protection in case there shall occur unexpected breakdown of air insulation, a metal oxide varistor was connected shunting the resistor. To reduce the noise interference level the measuring shunt resistance was enclosed in metallic box with effective shielding properties against electromagnetic interference. Meanwhile the corona emission signatures were captured using LeCroy oscilloscope LT344L 500-Mhz DSO. The scope has 4 channels for detection and measurement purposes, and a GPIB port for external connection with a computer for data transfer.

Figure 2.2 and Figure 2.3 depict the pictorial view of the experimental set-up and leakage current sensor box respectively.



(a)



(b)

C

Figure 2. 1 The novel air humidifier testing system, (a) Schematic diagram of the controlled room, and (b) The experimental set-up of corona emission.

HV Transformer  
240V/100kV



(a)



(b)

Figure 2. 2 Pictorial view of test set-up, (a) Front, (b) Right



Figure 2. 3 Pictorial view of leakage current sensor box

### 2.3 Experimental Procedures

Corona discharges are best investigated using rod to plane electrode configuration where the rod radius is chosen according to the field non-uniformity desired. For the negative DC voltage three modes of corona discharges are involved that is onset streamer, negative glow, and pre-breakdown streamer. In this case the pre-breakdown streamer mechanism was studied. The general characteristic of the discharge current is in the order of tens of nanoseconds for the front time, whereas the tail time is in the order of 100 nanoseconds, and pulse repetition rate is in the order of kHz.

Figure 2.2 shows the various types of LATs used in the experiments. Each electrode in turn was placed beneath the HV side plane electrode.



Figure 2. 4 Various types of LAT

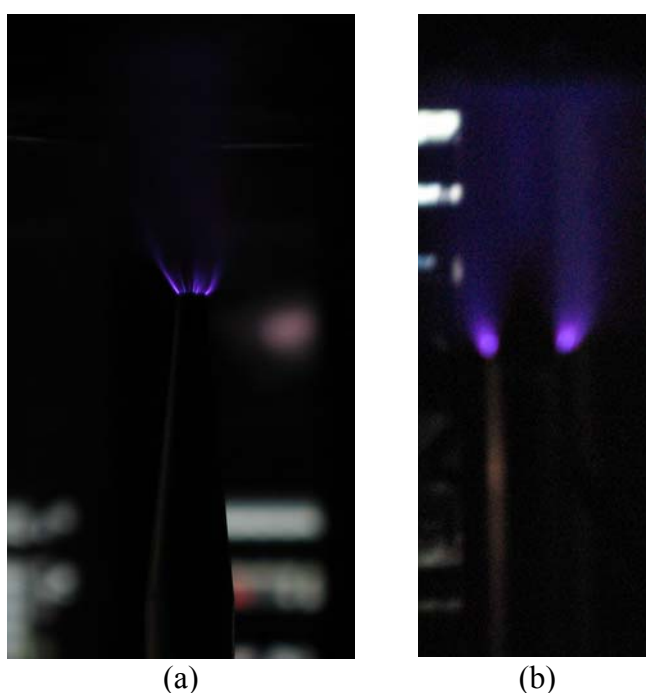


By gradually increasing the power frequency main voltage, affect the output high voltage DC and when continuous discharge of pre-breakdown streamer commenced after the emergence of negative glow and onset streamer, the voltage increment was stopped. At this point of time, the output voltage of the resistive divider and the peak corona discharge current was observed and recorded.

The observations of the corona discharge current were conducted with the attachment of LATs under test to the experimental rig grounding system via a 1.2-k $\Omega$  resistor. Therefore for 1-V measured across the resistor corresponds to 0.833-mA of corona discharge current. For surge protection in case there shall occur unexpected breakdown of air insulation, a metal oxide varistor was connected shunting the resistor. To reduce the noise interference level the measuring shunt resistance was enclosed in metallic box with effective shielding properties against electromagnetic interference.

## 2.4 Results and discussion

The photographic details of the corona discharges patterns can be seen in Figure 2.3.



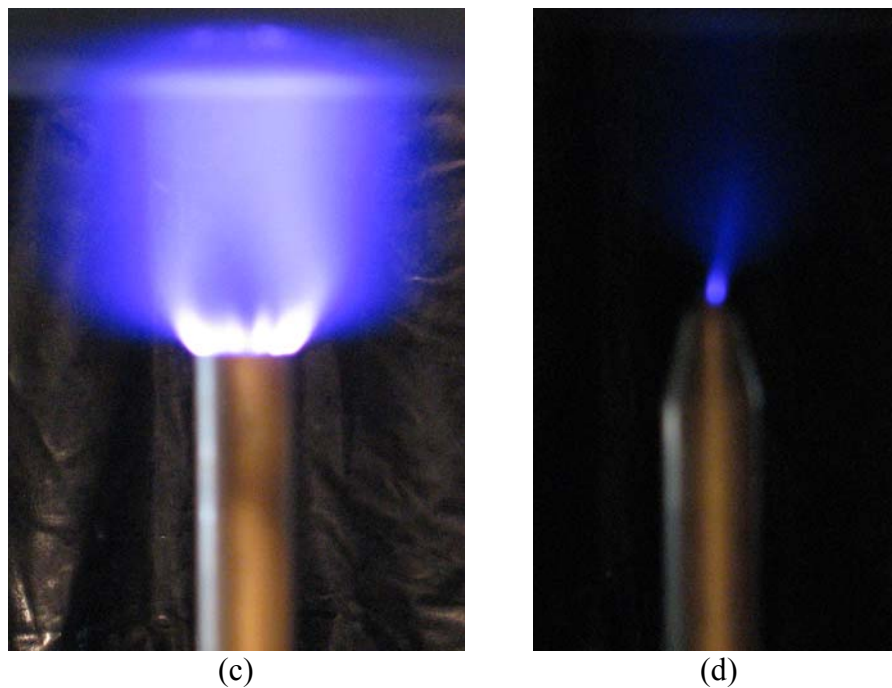


Figure 2. 5 Corona discharge on LAT tips, (a) standard, (b) concave, (d) flat, and (e) conical.

The results of corona discharge patterns show that they depend on the area that form shape edges. In this paper, afterwards, it will be mentioned as the area of tip that produces corona discharge ( $A$ ). Figure 2.4 shows the highlighted area of the LAT tips.

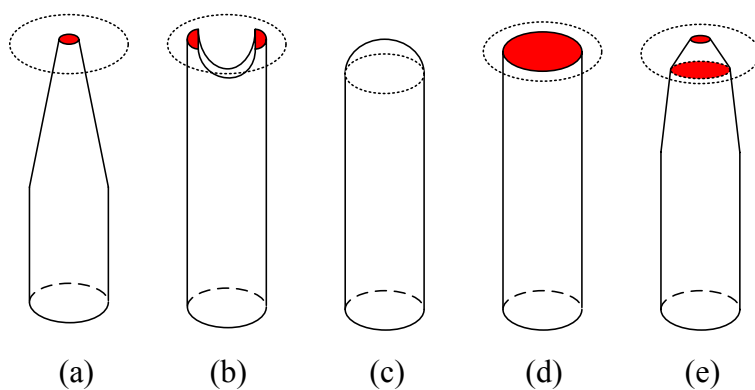


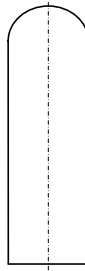

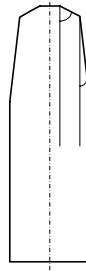


Figure 2. 6 The area of LAT that produce corona discharge current.

It is obvious that the corona discharge current will not occur on the blunt LAT because  $A$  is zero.

Closer analysis of tips' profile show the included angle of the tip could be a parameter for classifying the severity of pre-breakdown streamer activities as shown in Table 2.1.

Table 2.1 Tips' Profile Of LAT

The LATs					
Included angle (°)	$90+\alpha$	$90+\beta$	0	90	$90+\delta+\gamma$
Area (mm <sup>2</sup> )	12.57	0.85	0	37.70	21.99

## 2.5 Dimensional analysis

In engineering fields there are many particular applications employ empirical results from lots of experiments. The obtained data is frequently not easy to present in a comprehensible form and it may be difficult to interpret. Dimensional analysis can give a solution in selecting appropriate data and how it ought to be presented.

In all experimentally based areas of engineering, dimensional analysis is a quite useful procedure. It can provide the general forms of equation that describe natural phenomena. Its applications as conceptual tool are utilised in nearly all field of engineering to understand physical circumstances which is involving a combination of dissimilar kinds of physical quantities. If the involved factors in a physical situation is possible to be acquired, dimensional analysis can be utilised to form a relationship between them [45].

This section describes the development of a mathematical model by using dimensional analysis to obtain the closed loop equation. The corona discharge current ( $I_{cd}$ ) depends on a number of parameters that have significant contribution. The important amongst them are permittivity ( $\varepsilon$ ), time ( $T$ ), area of tip that produce corona ( $A$ ), distances ( $d$ ), and input voltage ( $V$ ). A mathematical relationship between the  $I_{cd}$  and the parameters can be presented in the form,

$$I_{cd} = I_{cd}(\varepsilon, T, A, d, V) \quad (1)$$

When the parameters in equation (1) are written in terms of four fundamental dimensions; length ( $L$ ), mass ( $M$ ), time ( $T$ ), and electric charge ( $Q$ ), the corresponding dimensional matrix is

$$\begin{array}{c|cccccc} & I_{cd} & \varepsilon & T & A & d & V \\ M & 0 & -1 & 0 & 0 & 0 & 1 \\ L & 0 & -3 & 0 & 2 & 1 & 2 \\ T & -1 & 2 & 1 & 0 & 0 & -2 \\ Q & 1 & 2 & 0 & 0 & 0 & -1 \end{array} \quad (2)$$

The rank ( $r$ ) of dimensional matrix is 4, and the number of parameters ( $n$ ) is 6. According to Buckingham- $\pi$  theorem a solution can be presented as  $(n-r) = 6 - 4 = 2$  independent dimensionless product ( $\pi_x$ ). Then the dimensional matrix can be written in the form:

$$\begin{array}{c|cccccc} & \zeta_1 & \zeta_2 & \zeta_3 & \zeta_4 & & \\ & I_{cd} & \varepsilon & T & A & d & V \\ M & 0 & -1 & 0 & 0 & 0 & 1 \\ L & 0 & -3 & 0 & 2 & 1 & 2 \\ T & -1 & 2 & 1 & 0 & 0 & -2 \\ Q & 1 & 2 & 0 & 0 & 0 & -1 \end{array} \quad (3)$$

where  $\zeta_1, \zeta_2, \zeta_3$ , and  $\zeta_4$  are the indices of the variables in equation (1) as repeating variables.

The dimensional expression for  $\pi_1$ , and  $\pi_2$ ;

$$\pi_1 = I_{cd}^{\xi_1} \varepsilon^{\xi_2} T^{\xi_3} A^{\xi_4} d \quad (4)$$

$$\pi_2 = I_{cd}^{\xi_1} \varepsilon^{\xi_2} T^{\xi_3} A^{\xi_4} V \quad (5)$$

As the  $\pi$  groups are all dimensionless  $M^0L^0T^0Q^0$  the principle of dimensional homogeneity to equate the dimensions for each  $\pi$  can be used. Then a set of dimensionless products are introduced.

$$\pi_1 = A^{-0.5} d \quad (6)$$

$$\pi_2 = I_{cd}^{-1} \varepsilon T^{-1} A^{0.5} V \quad (7)$$

According to Buckingham's Theorem, the dimensionless parameters are related by function

$$\phi(\pi_1, \pi_2) = 0 \quad (8)$$

Finally, the model of corona discharge current can be presented as:

$$I_{cd} = D_c \left( \frac{\varepsilon AV}{Td} \right) \quad (9)$$

where  $D_c$  is a dimensionless constant that will be determined from the experiments.

The peak to peak of corona discharge current average against the HV input per centimetre of distance and the corona discharge current model for standard, concave, flat, and conical LATs are shown in Figure 2.7 to Figure 2.10. The uncertainty ranges are within  $\pm 0.5$ -mA. Corona discharge current developed on the blunt LAT, however, was so small which can be neglected. The model and the experimental results are in agreement.

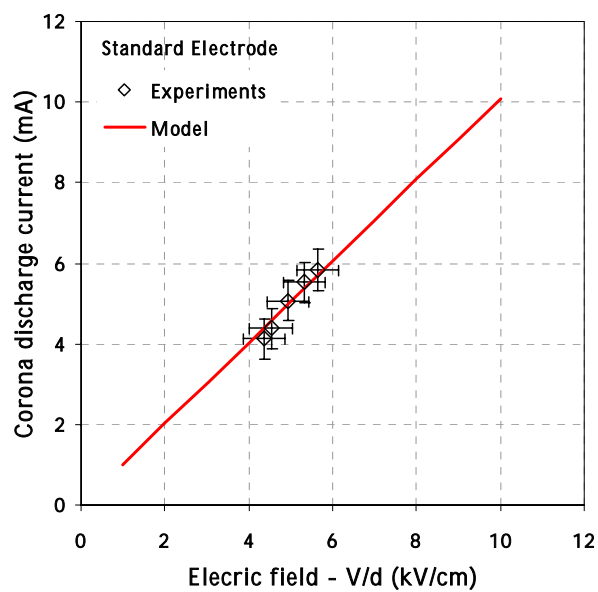


Figure 2. 7 Electric field versus corona discharge current of Standard LAT.

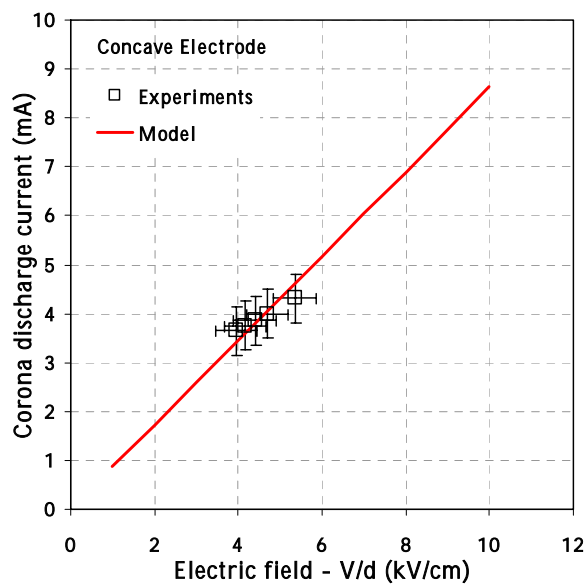


Figure 2. 8 Electric field versus corona discharge current of Concave LAT.

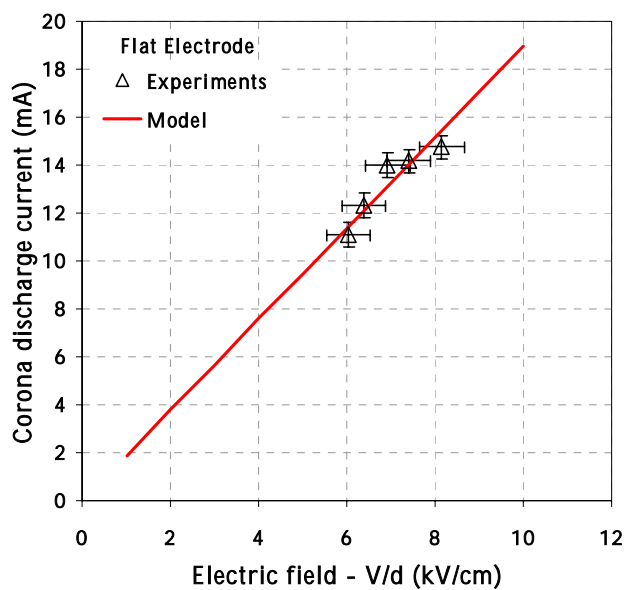


Figure 2.9 Electric field versus corona discharge current of Flat LAT.

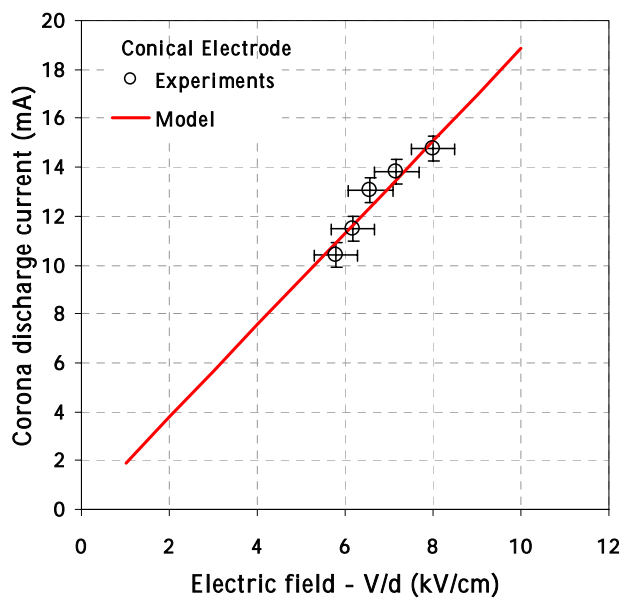


Figure 2.10 Electric field versus corona discharge current of Conical LAT.

From results as shown in Figure 2.7 – 2.10 corona discharge currents at the electric field of 6-kV/cm is determined. This is to observe the correlation of the sharp

edges areas of LAT with the corona discharge currents. Figure 2.11 shows the obtained results.

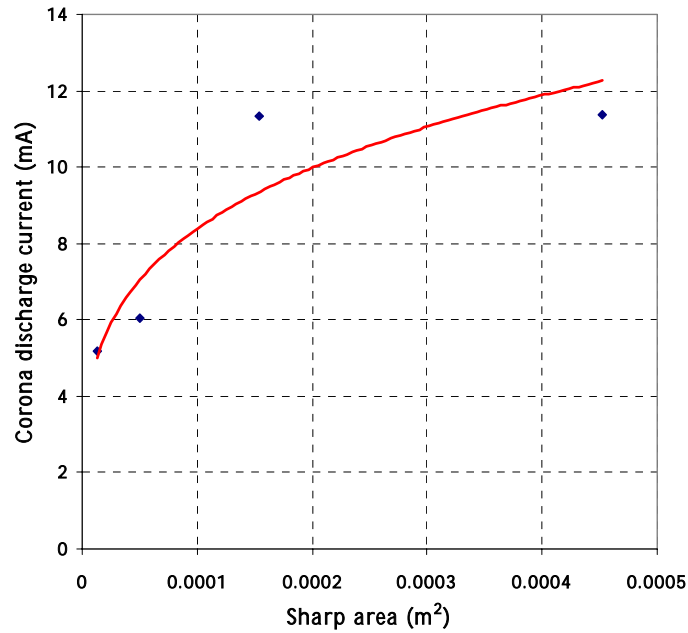


Figure 2.11 Obtained results of 6-kV/cm electric field and the corona discharge current.

As shown in Figure 2.11 the corona discharge currents increase along with the increment of sharp areas. By using the regression method the constant that influence the  $A$  can be determined as given in equation (10).

$$I_{cd} = 84.579 \left( \frac{\varepsilon V A^{0.2508}}{Td} \right) \quad (10)$$

## 2.6 Conclusion

From the observation of the corona discharge a new closed loop mathematical modelling has been developed by applying dimensional analysis which can simulate the magnitude of corona discharge currents involved. The standard Franklin rod used in this work is a typical Franklin rod practically installed in Malaysia. Again, the



finding strengthened the fact that for better capturing of lightning leaders, blunt tip LAT is preferable.

## **CHAPTER 3**

### **DEVELOPMENT OF INDIGENOUS ELECTRIC FIELD MILL FOR EARLY WARNING AND TRIGGERING LASER SYSTEM**

#### **3.1 Introduction**

The atmospheric electricity is affected by clouds in atmosphere where characteristically every cloud types have different electrical effects [46]. The clouds will be formed when the ambient humidity attain a certain threshold value and followed by an updraft. Moisture concentration density in a particular area is probably a major contribution to ambient humidity level variation. Meanwhile the occurrence of updraft basically due to the Earth's surface sunlight heating and the wind flows through hills, mountains, or land surface contours. There are four mechanisms that cause air to rise [47]. Firstly, the orographic lifting where air is forced to rise over a mountain barrier. Secondly the frontal wedging where the warmer, less dense air, is forced over cooler, dense air. Thirdly, the convergence is a pileup of horizontal air flow results in updraft movement. Fourthly, the localized convective lifting is an unequal surface heating that causes localized pockets of air to rise because of their buoyancy.

Another important thing involved in the cloud formation is the existence of hygroscopic nuclei. The hygroscopic nuclei are becoming the nuclei of water molecules in clouds as a result of a condensation process. Relying on the geographic situations, the typical of hygroscopic nuclei can vary amongst the regions. They can

be microscopic dusts from coal mining, salt particles from oceans, smog from industries, and others [47].

The different types of clouds are results of different meteorological conditions. A lot of useful information pertaining to the daily weather can be acquired by observing the clouds. For describing their appearance clouds are named by using Latin prefixes and suffixes. Clouds can generally be classified into four main categories regarding to their shape and height [47-52].

1. High clouds, it is above 6000-m consist of ;
  - a. Cirrus clouds are wispy, delicate, fibrous, white, and thin clouds usually associated with fair weather, but may indicate approaching bad weather in the nearby occasion. Cirrus clouds are composed of ice crystals or supercooled water that come from frozen water droplets.
  - b. Cirrocumulus clouds are thin, and white. They are ice-crystal clouds possibly will look like ripples, waves, or rounded masses all in a row. Commonly linked with fair weather, but may indicate that storms will occur in the near future. A mackerel sky may be produced by these clouds existence.
  - c. Cirrostratus clouds are white thin sheet-like clouds or veil-like clouds which are composed of ice-crystal that possibly will show a milky sky. Occasionally these clouds cause halos to appear around the Moon or Sun. These clouds usually associated with fair weather, but they existence may indicate approaching storms. Though cirrostratus can obscure the sky due to their many thousands of metres thick, cirrostratus are moderately transparent. Therefore the Moon and Sun are usually observed through cirrostratus.
2. Middle clouds of height 2,000-6,000-m consist of;
  - a. Altocumulus may be found as light grey clouds which are frequently composed of separate patches or rolls. They are often established before rain or thunderstorms. Usually altocumulus clouds are darkness is distinguish them from cirrocumulus.
  - b. Altostratus clouds are generally thin grey or bluish fibrous clouds. They may produce very light continuous precipitation, and indicate approaching warmer weather. Altostratus clouds may cause the Sun or Moon appearance as a bright spot, but they may not produce halos.

3. Low clouds of height below 2,000-m consist of;
  - a. Stratocumulus clouds are low lumpy layer clouds with some vertical structure in which are vary in colour, from dark grey to soft grey. These clouds are in globular patches or rolls that may form a continuous layer with breaks of clear sky in amongst. Infrequently weak rainfall and snow are produced from these clouds.
  - b. Stratus clouds are low uniform horizontally layer form dark, dull grey, cover the entire skies that may continue for days and associate with drizzle. These clouds are similar to fog but not touching the Earth's surface.
  - c. Nimbostratus clouds are stratus clouds, in which are associated with continuing light to moderately falling precipitation. These clouds are one of the main precipitation-producing clouds from which rain or snow falls. Their layers are thick and dark as the result they may obscure the Sun or Moon. Ice particles and snow may be created in these clouds when a particular temperature is attained.
4. Clouds of vertical development, within 500-18,000-m
  - a. Cumulus clouds are dense, puffy white, and heap clouds that look like heads of cauliflower with flat bases. Commonly these clouds are associated with fair weather. However they will possibly produce precipitation if there is great vertical development. The top of cumulus clouds may be reach 10-km or even more above their bases on the hot summer season.
  - b. Cumulonimbus clouds are towering rain clouds occasionally outspreading on uppermost to develop an anvil head. These clouds will possibly be followed with heavy rainfalls, thunderstorms, lightning, hail, and tornadoes. The uppermost of cumulonimbus clouds may arise to the stratosphere. Usually heavy brief rains are developed from these clouds. The cumulonimbus clouds are the primary source of lightning. However, regarding to Rakov [53] not every cumulonimbus cloud produces lightning. Therefore he preferred

to define the thunder cloud as “lightning-producing cumulonimbus” instead of merely “cumulonimbus”. This is better to avoid redundant.

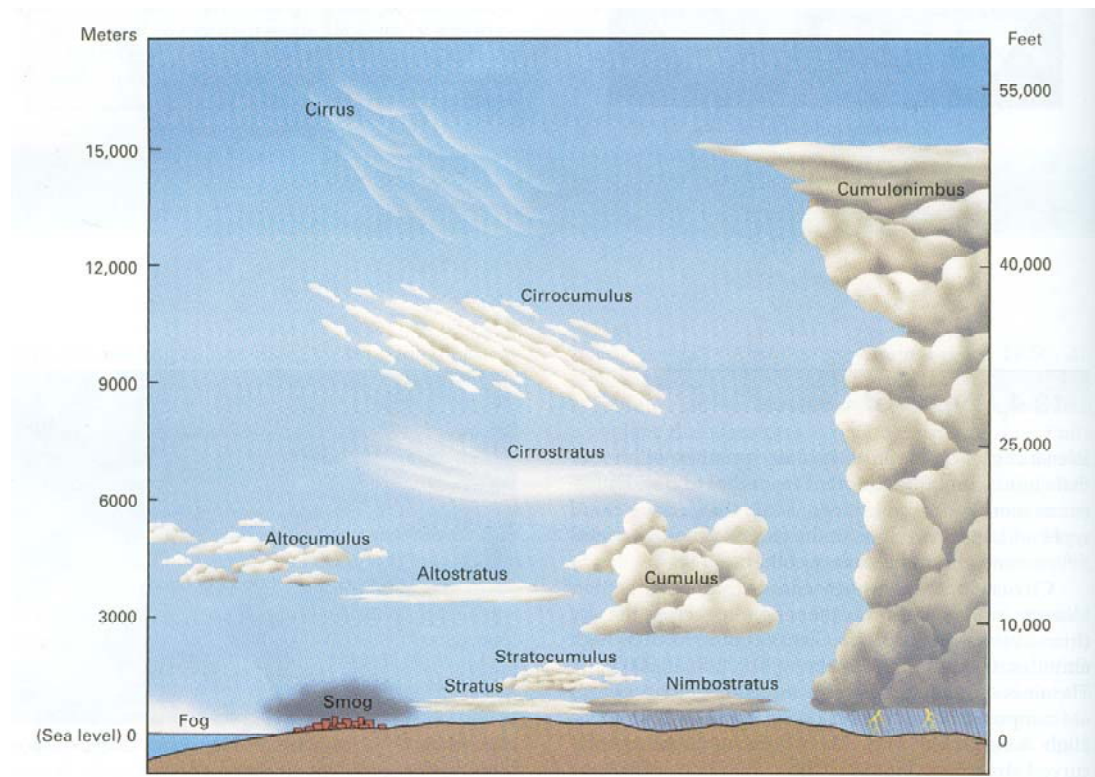


Figure 3.1 Cloud's names are based on the shape and the altitude of the clouds [48].

### 3.2 Thunderstorm Formation And It Electrification Process

A thunderstorm is a peculiar type of storms that produces lightning and thunders, followed by gusty winds, heavy rain, and hail. A single (influence only for a small region) or clusters (covering a large region) of thunderstorm-producing cumulonimbus cloud can generate a thunderstorm. In the tropical region where warmth, abundance of moisture, and unstable environmental condition are constantly present, causing the greatest numbers of thunderstorms. There are many mechanisms that can lead to the updraft movement necessitating the development of thunderstorm-producing cumulonimbus.

Generally, a typical thunderstorm is developed in three phases [47,48]. The early phase involves the condensation process of the moisture rising air, thus

developing a cumulus cloud. Because of the cloud formation the condensing vapour releases sufficient latent heat to sustain its upward movement and therefore the air inside the cloud becomes warm and promotes the convective characteristics of the thunderstorm. Within this phase large water droplets or ice crystals have developed. However, the rising air keeps them in suspension and precipitation does not occur. Finally, when the water droplets and hailstone become too heavy as such the updraft movement cannot longer support them, as a result they fall as rain or hail. During this phase, the warm air in the central and upper parts of the cloud, keep on rising and its velocities probably reaches over 300-km per hour. In just few minutes the cloud may double in height. Simultaneously, ices descend down toward the lower part of the cloud experiencing cooling and this cool air falls, develop a downdraft. On this account, air flows upward and downward concurrently within the same cloud. The mature stage of a thunderstorm takes place within 15 to 30 minutes but sometime for an hour. The mature stage will be attained due to the amount and size of accumulated-precipitation is excessively for the updraft to continue, whereas in another part of the cloud the downdraft happens that is producing heavy precipitation. This is the most active phase of the thunderstorm, resulting gusty winds, severe lightning, heavy precipitation, and sometime hail or even tornadoes. Eventually the cool downdraft decreases the temperature in the lower parts of the cloud. Moist air is no longer changed into the cloud. The storm loses its source of latent heat because of stopping in condensation. In a few minutes the rapid vertical air movement ceases and the storm disperses. Even though a single thundercloud can disperse rapidly, new thunderheads are able to build in the same region.

A thunderstorm-producing cumulonimbus clouds mostly produce lightning. Lightning is an intense electrical discharge that is resulted by the cloud electrification process associated with the process mentioned earlier. The lightning discharges occur when the insulating properties of air cannot attain anymore the accumulation of static electricity of the clouds [48]. In conjunction with the accumulation, many efforts have been made to understand the mechanism of cloud electrification process. Yet the phenomenon of charges separation into different area in the thunderstorms-producing cumulonimbus cloud is not fully understood. There are many theories presented regarding the cloud electrification mechanism [53-56]. Accordance with Rakov and Uman [53] the dominant mechanism is the graupel-ice mechanism. This mechanism presents at least at the early stages of cloud electrification process.

### **3.3 Electric Field Strength**

The ambient electric field strength gives information about the lightning incidence. According with Jacobson [56], when the electric field strength, due to the presence of clouds, is over the limit of ambient air insulation threshold, lightning will occur where the range generally is from  $1\text{-kVcm}^{-1}$  to  $4\text{-kVcm}^{-1}$  or within average of  $3\text{-kVcm}^{-1}$ . Meanwhile without the presence of clouds the electric field strength near the Earth's surface is only about  $1.3\text{-kVcm}^{-1}$ . In the absence of clouds, the Earth's surface is charged slightly negative and the upper atmosphere is charged slightly positive.

To measure the ambient electric field strength or potential gradient various methods have been introduced [46]. One of which is the Electric Field Mill (EFM). However, in some circumstances the Rotating-vane EFM (REFM) is generally being used as an instrument for observing the cloud electrostatic phenomena. The principles of operation and locations determination of REFM are being widely studied by many authors [57 – 61].

### **3.4 Indigenous Rotating -vane Electric Field Mill**

Following the necessity to develop a new LAT that is equipped with laser-triggering system (Laser Aided Radiation Ionisation Process), an in-house REFM is required to be developed. Some benefits will be obtained by this development especially in conjunction with the customisations of the instrument. Interestingly another additional benefit, however it is not the purpose, is lessening the burdens of cost.

### **3.4.1 General Principle of the REFM**

The REFM is an induction field meter with which the ambient electric fields strength can be measured. This instrument consists of a grounded rotating-vane positioning in front of a sensor plate. Since the rotating-vane turns, and therefore the sensor plate will be alternately exposed to and shielded from the induction field; an AC signal will be generated on the sensor plate because of that continuing process.

Similar to the other instrumentations, the REFM must be calibrated before applied to the real measurements. A known DC voltage source positioning in various distances from REFM is usually used to calibrate the REFM.

### **3.4.2 Developed REFM**

The depiction of the developed REFM is given in Figure 3.2. It consists of a rotating-vane, a sensor plate, and a 12-V DC motor inside the chamber. The rotating-vane and the sensor plate are made equivalently in dimension and shape. Then to fasten the rotating-vane at the motor shaft a special coupling unit is also designed. The gap distances amongst of the rotating-vane, the sensor plate, and the upper part of motor chamber are arranged equally in 1-cm.





Figure 3.2 Rotating-vane type EFM

All these component designs also consider the possibility of corona development on the edges of the every component. Since the REFM is applied in high intensity electric field, these four component edges are made as blunt as possible to reduce the possibility of corona development. The corona development on the edges of REFM for a long time application can significantly alter the component shapes.

Hence, beside the physical design as mentioned previous, the material selection is an important thing to consider since the REFM will be placed outdoor. Concerning the harsh outdoor vicinity the original stainless steel material is the most suitable material for this work. This kind of material is corrosion-free and very tough.

### 3.4.3 Signal Processing

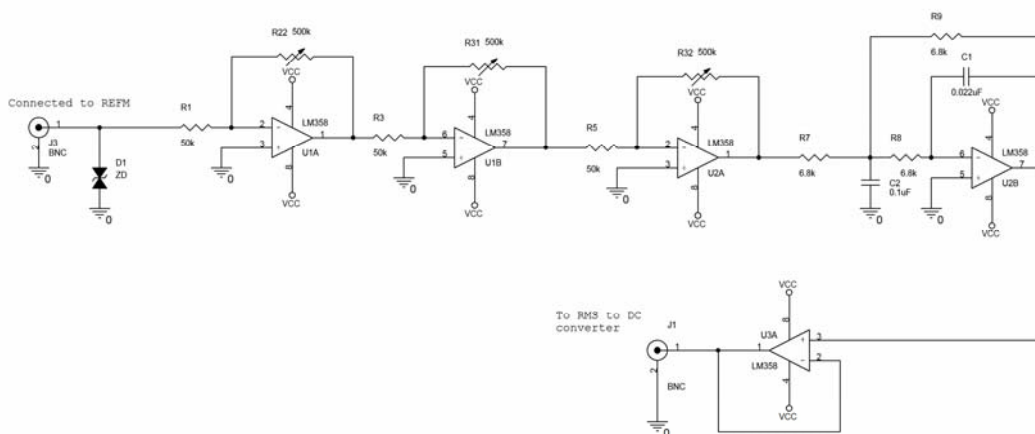
The signals generated from the sensor plate must be processed to obtain good quality of electric signals. The signal processing terms involve the amplification, filtering, conversion, and harmonization. The amplification process is housed in an

independent unit while the filtering, conversion, and harmonization part are placed in another separate unit.

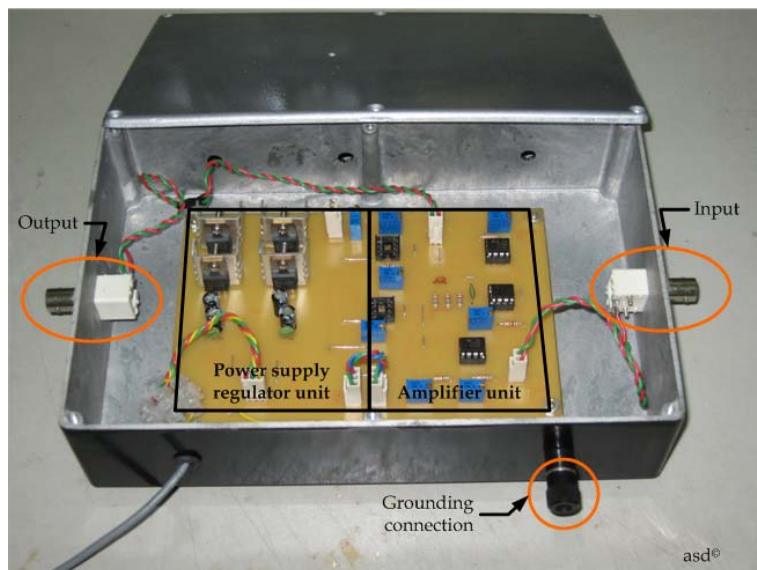
### 3.4.3.1 Amplification unit

Actually, the induced-voltage on the sensor plate is too small in magnitude to be observed directly; hence a signal amplification unit is necessary. For this, three-stage signal amplification system is developed with the total amplifications are about one-thousand times. This electronic part is energized with a 12-V DC regulated power supply which is developed indigenously.

This signal amplification unit is placed in a secure aluminium box which is facilitated with a grounding connection outlet. By grounding the box unwanted signals infiltration to the electronic system due to the electromagnetic radiation process can be eliminated. The metal enclosure protects the electronic circuits from electromagnetic interference. Figure 3.3 and Figure 3.4 shows the system amplifier and the waveform output respectively.



(a)



(b)



(c)

Figure 3.3 The signal amplification unit, (a) Schematic diagram, (b) Amplifier board, and (c) Aluminium box.

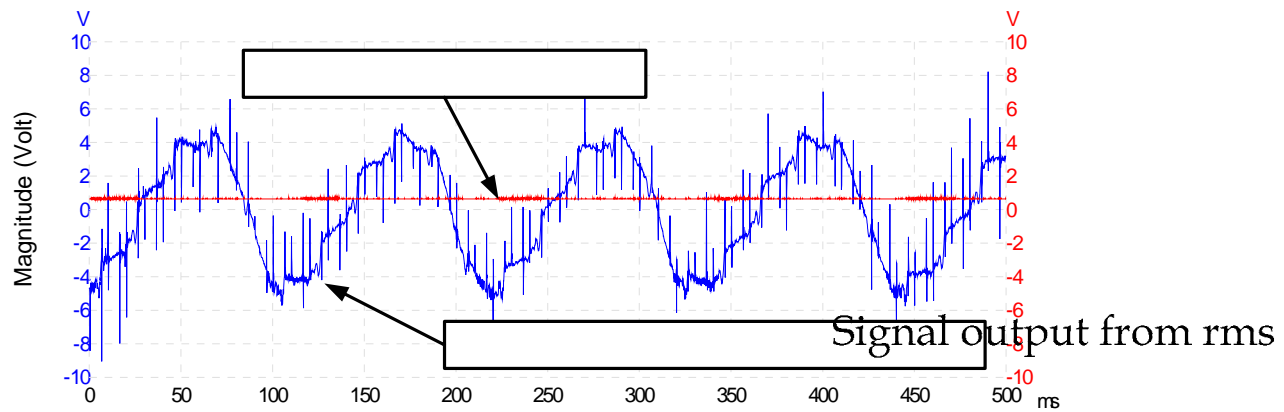


Figure 3.4 The output of signal amplification unit

### 3.4.3.2 Filtering, Conversion, and Conditioner Unit

After the amplification process the signal is filtered. The objective is not only to pick selected part of signal harmonic but also to remove unwanted noises. In this work the filter is of a first-order passive low-pass filter placed after the amplification unit. The application of filtering system causes the signal magnitude to decline.

For this application the declination is also an important consideration since the output from the filter will feed the AD536. The function of AD536 is to perform a true rms to dc signal conversion. It is a complete monolithic integrated circuit which directly computes the true rms value of any complex input waveform containing ac and dc components.

Figure 3.5 shows a simplified schematic of the AD536 [62]. It is subdivided into four major sections: absolute value circuit (active rectifier), squarer/divider, current mirror, and buffer amplifier. The input voltage,  $V_{IN}$ , is rectified and converted to a unipolar current  $I_1$ , by the active rectifier A1, A2.  $I_1$  drives one input of the squarer/divider, which has the transfer function:  $I_4 = I_1^2/I_3$ . The output current,  $I_4$ , of the squarer/divider drives the current mirror through a low-pass filter formed by R1 and the externally connected capacitor,  $C_{AV}$ . If the R1,  $C_{AV}$  time constant is much greater than the longest period of the input signal, then  $I_4$  is effectively averaged. The

current mirror returns a current  $I_3$ , which equals  $Avg. [I_4]$ , back to the squarer/divider to complete the implicit rms computation. Thus:  $I_4 = Avg.[I_1^2/I_4] = I_1 \text{ rms}$ . The current mirror also produces the output current,  $I_{OUT}$ , which equals  $2I_4$ .  $I_{OUT}$  can be used directly or converted to a voltage with R2 and buffered by A4 to provide a low impedance voltage output. The transfer function of the AD536 thus results:  $V_{OUT} = 2R_2 I \text{ rms} = V_{IN} \text{ rms}$ .

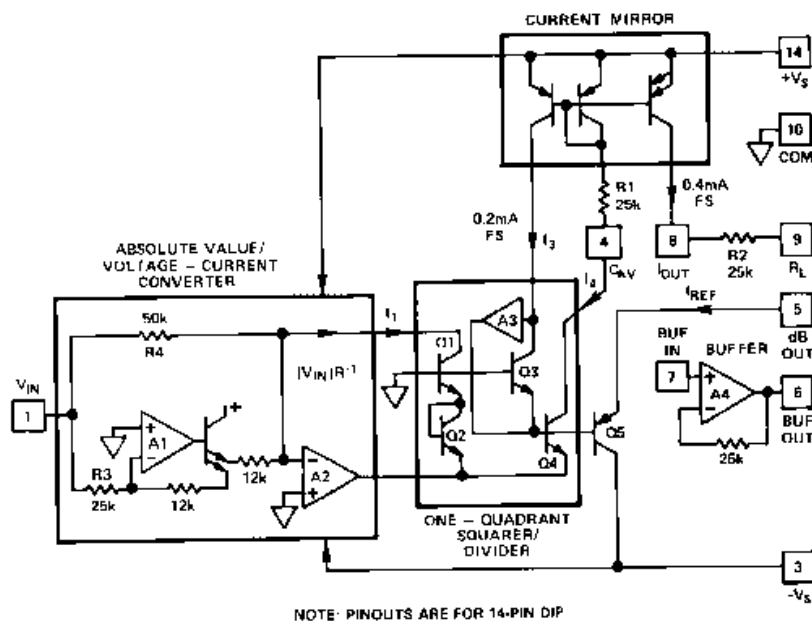
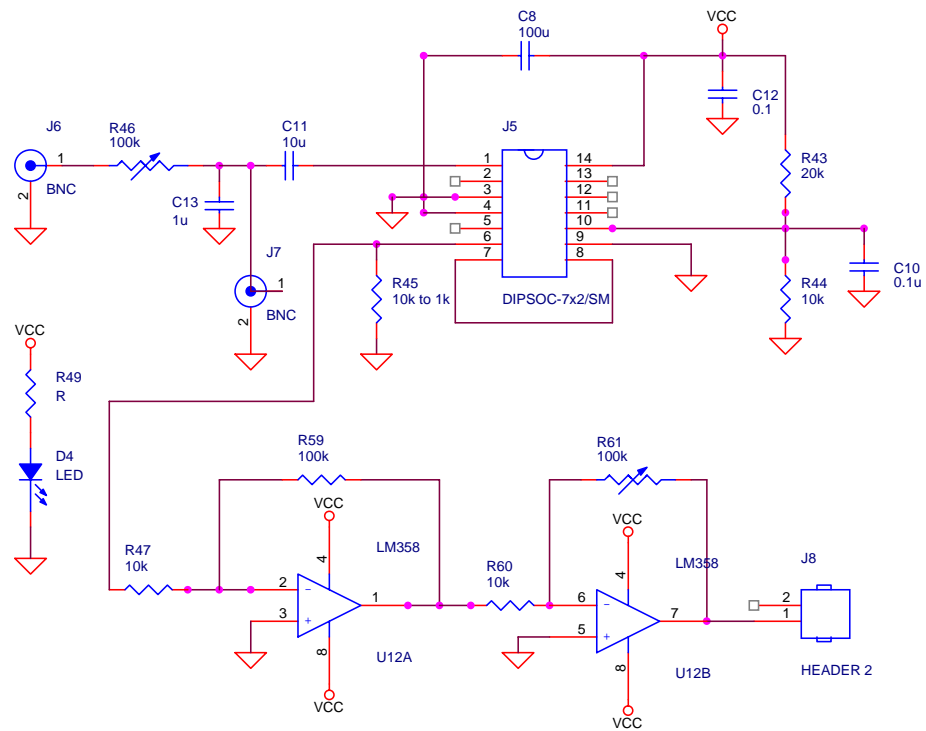
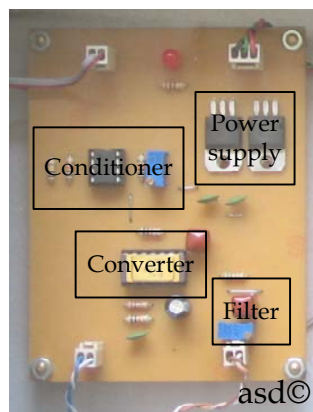


Figure 3.5 Simplified schematic of AD536

The output signal from the AD536 in the next stages will be used to feed a microcontroller. As normally application prescriptions any input signal to the microcontroller must be conditioned to a certain magnitude so that they will not damage the microcontroller. Pertaining with signal conditioning between the AD536 and the microcontroller, an operational amplifier LM358 is used for this purpose. The schematic diagram and electronic circuit of the filter, converter, and conditioner unit are illustrated in Figure 3.6 whereas the sample of the signal output is given in Figure 3.7.



(a)



(b)

Figure 3.6 The filter, converter, and conditioner unit, (a) schematic diagram and (b) electronic circuit

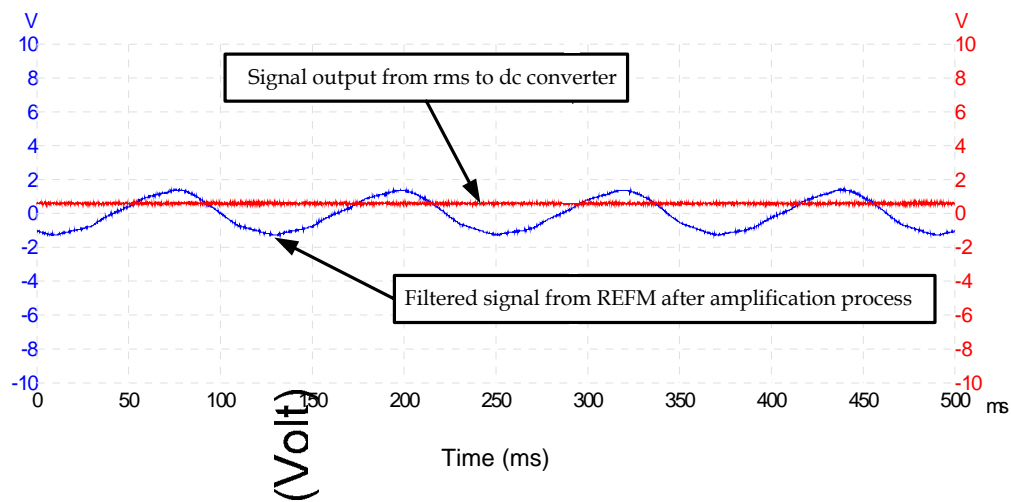


Figure 3.7 The sample of signal output from

#### 3.4.4 Microcontroller Unit

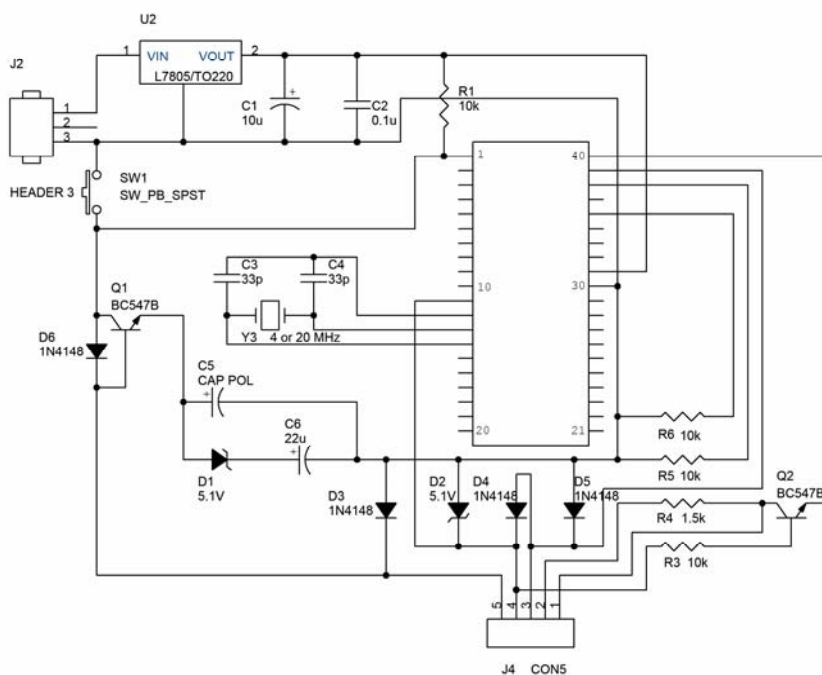
A microcontroller unit is a highly integrated circuit (IC) which has similar function with a general-purpose computer system. Hence, generally a microcontroller contains a CPU, RAM, ROM, I/O peripherals, and timers. It is designed to be applied for a very specific task. A system using a microcontroller can be simplified and reduced in dimension.

In applications where numerous decisions or calculations are necessary, microcontrollers are very practical. The microcontrollers can be programmed according to the user necessity by using software(s). The applications of software base computational, in most cases, are easier than discrete logic. Moreover it can replace complex and expensive hardware components.

This current work uses a PIC16F778A microcontroller which is also equipped with a built-in analog to digital converter (ADC) unit. The ADC unit is needed because a microcontroller can only receive digital signal for its operation. Instead of using a microcontroller without built-in ADC unit in which an independent ADC must be developed, the applying of microcontroller with a built-in ADC is less demanding. This PIC16F778A microcontroller is operated with a 5-V regulated DC power supply.

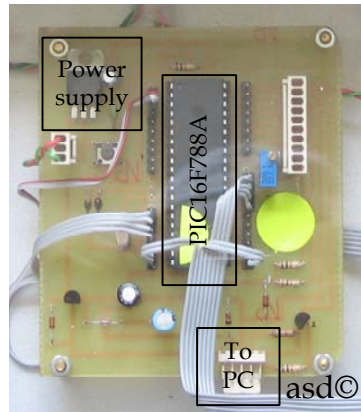
In order to operate the microcontroller according to certain responds, an algorithm must be embedded into the microcontroller. The algorithm should be translated to a program code. In this present work, the program code is written by using C language.

By using an emulator device, the program code is embedded to the microcontroller. The emulator can be a separated unit or be integrated to the microcontroller unit. The latter enables the embedding process with microcontroller is still attached on the unit.



(a)



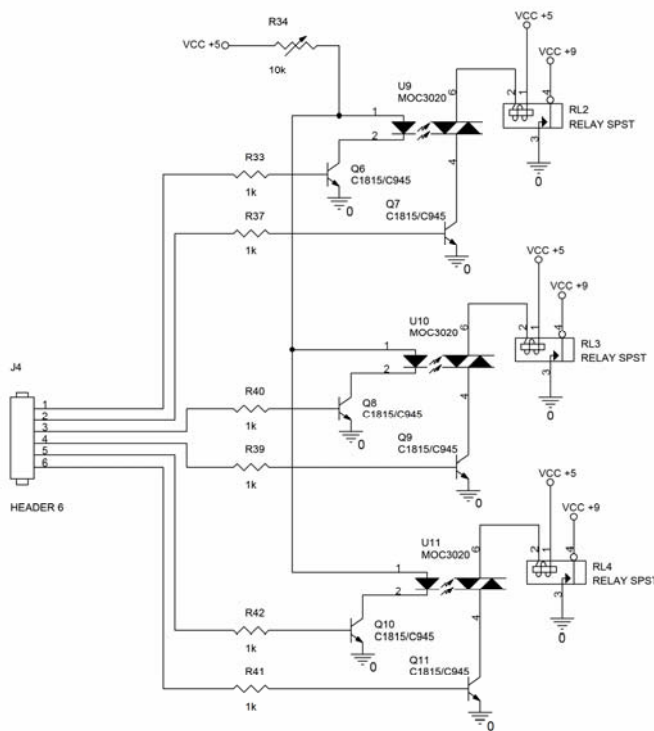


(b)

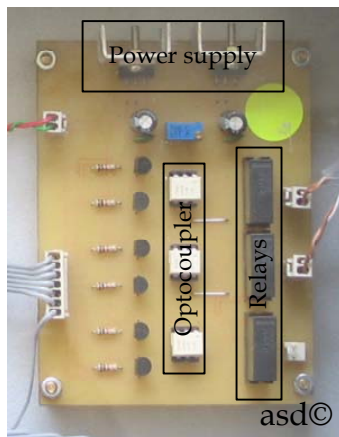
Figure 3.8 The microcontroller unit integrated with the emulator circuit, (a) Schematic diagram and (b) Circuit board

### 3.4.5 Relay Board Unit

A relay board unit is designed with a three-output channel incorporated with optocouplers that is used as interfacing unit between the relays and microcontroller unit. The utilization of optocoupler is to provide more reliable protection to the microcontroller unit from back EMF effect that is produced by the relays. These relays are employed as switch to activate an early warning system unit and a laser triggering system; while a built-in power supply is provided by two units of DC voltage regulator with 5-V output. The relay unit schematic diagram and electronic circuit is shown in Figure 3.9.



(a)



(b)

Figure 3.9 The relay board unit, (a) Schematic diagram and (b) Electronic circuit

### 3.4.6 Integrated Unit

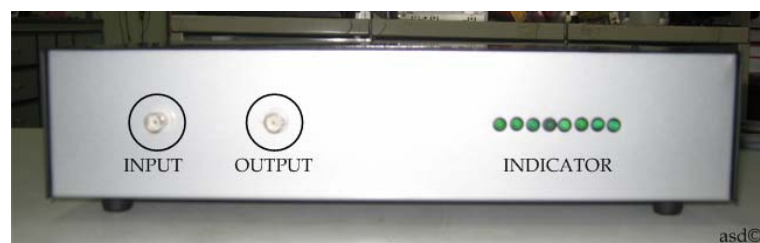
Each units that has been described above is combined to form a single integrated unit and being placed in a galvanize iron (GI) box as shown in Figure 3.10.

Figure 3.10 (a) shows the top view of the integrated unit on which the arrow signet shows the direction of flow of the input signal coming from the REFM. Its front view is presented in Figure 3.10 (b) showing input, output socket, and an eight LED indicator. Meanwhile, rear side of the box has two relay output sockets, power output socket, and power input cable are provided as shown in Figure 3.10 (c).

This integrated unit uses a single non-regulated DC power supply source that consists of a step down transformer (0.5-A, 240/18-V), and a 1-W bridge diode.



(a)



(b)



(c)

Figure 3.10 The integrated unit, (a) top view, (b) front view, and (c) back view

### 3.5 The REF M Calibration

## RELAY OUTPUT

The by product of this research is the construction of REF M which acts as sensor unit for the subsequent launching of laser beam. It is sensing the variation in the magnitude of cloud electric field. Upon the magnitude exceeding the lightning electric field prior to leader propagation, laser beam will be triggered. So a calibration process must be performed to acquire a mathematical equation that will be used as a correlation factor between the actual electric field in vicinity received by REF M and the output of the integrated unit.

#### 3.5.1 Methodology

The calibration exercise is performed in IVAT by using the same experimental setup employed in Chapter 2. However, in this occasion the sprinkler is not activated.

Figure 3.11 shows the REF M calibration setup where the REF M is placed beneath the cloud simulator (HVE) connected to the HVDC supply. The input voltage HVDC supply is controlled with a variable voltage regulator (VAR) device in the low voltage side.

Three distance settings are used in this calibration work, i.e. 30-cm, 48-cm, and 70-cm. The data collection is made online in which the increment of power

frequency input voltage to HV transformer from VAR ( $V_{in-trans}$ ) and output of the integrated unit ( $V_{out-int}$ ) are captured simultaneously. This process requires an analog to digital converter device. It is a PicoScope 3206 which is utilized as interface to a Note Book PC.

Since the PicoScope 3206 is rated at 20-V maximum input voltage, a HV differential probe (Tektronix P5200) is used to link the power frequency input voltage to the PicoScope. The actual configuration of the simulation cloud (HVE) and REFM is given in Figure 3.12.

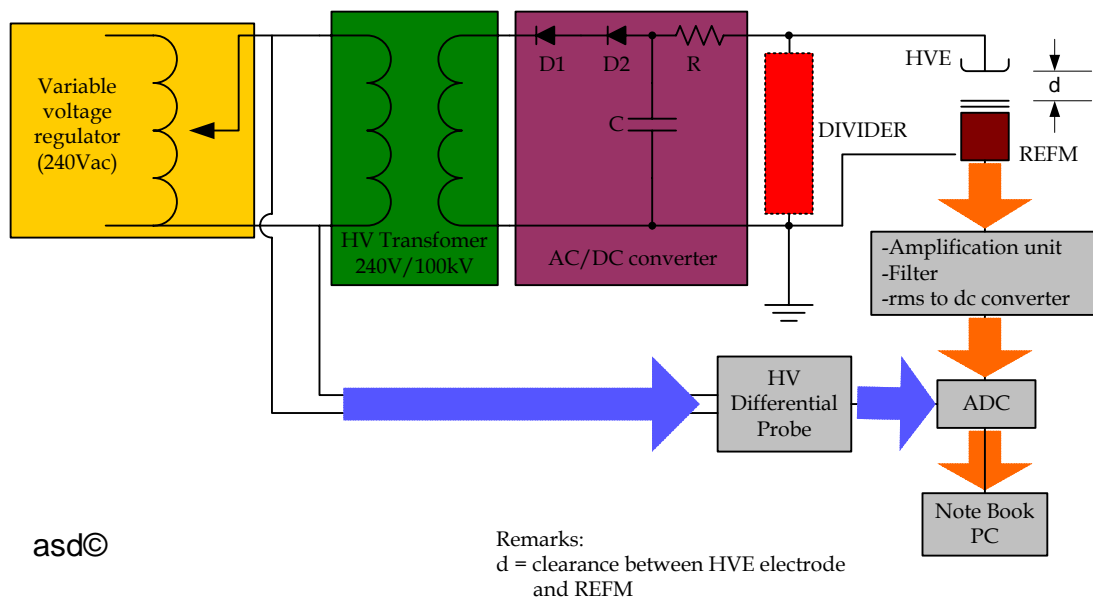


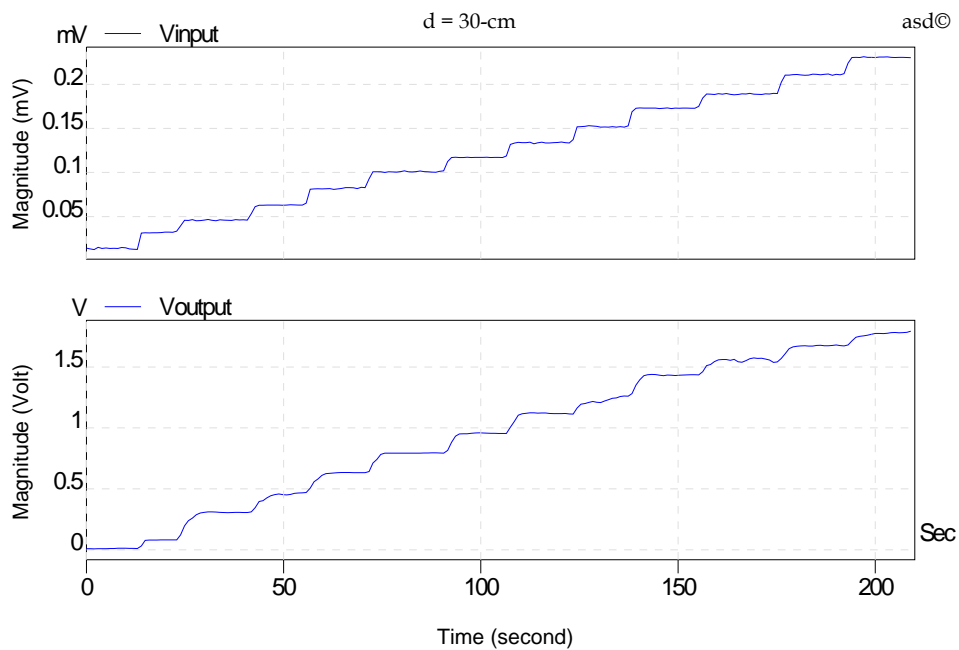
Figure 3.11 The general of REFM calibration setup



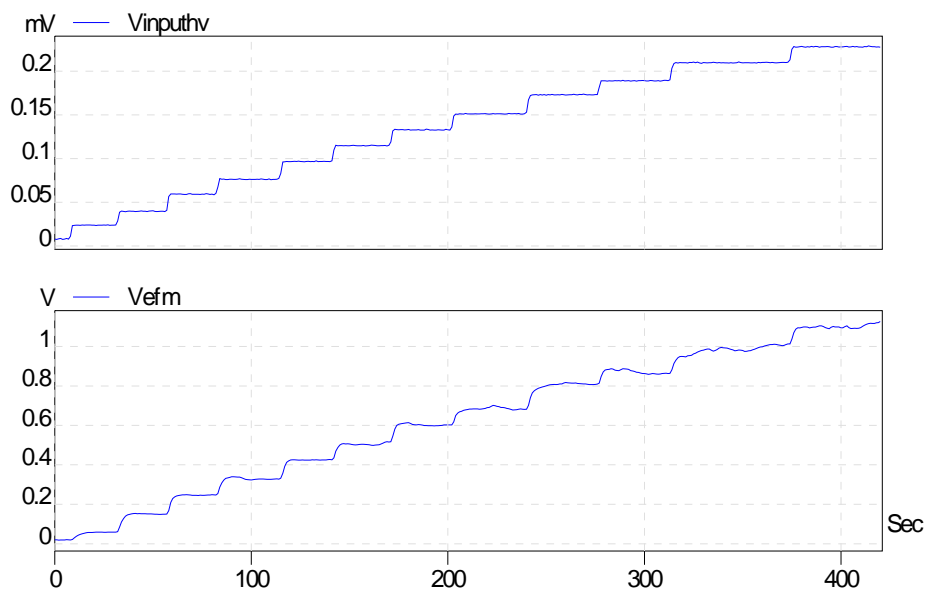
Figure 3.12 The REFEM calibration setup

### 3.5.2 Calibration Results and Discussion

The online measurement results of calibration work are shown in the Figure 3.13. The  $V_{in-tran}$  results must be correlated to the value of HVDC generator output. The correlation factor has been obtained by comparing the input voltage against the output of the HVDC generator which was made in calibration of the HV equipment.

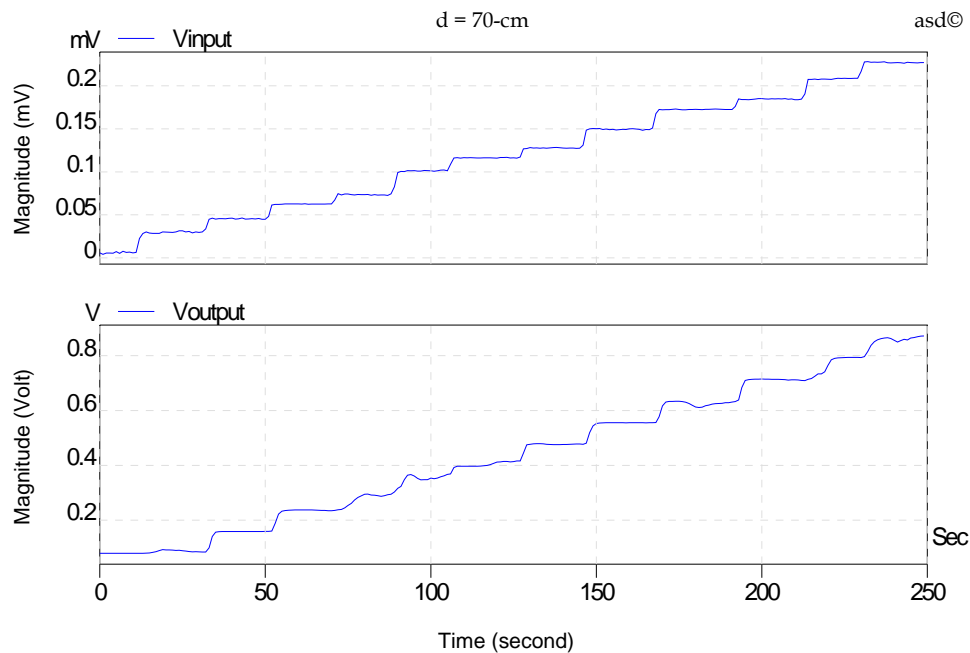


(a)



(b)

mV)



(c)

Figure 3.13 The results of online calibration measurement according to the distance of the cloud simulation to the REFm, (a) 30-cm, (b) 48-cm, and (c) 70-cm.

After the HVDC input voltages are obtained, mean the HVE voltage is known, the applied electric field strength on the REFm can be presented by dividing the HVDC input voltages with the distance between HVE and REFm. The detailed data presenting the correlation between electric fields strength on the REFm and the output of the integrated unit is given in Figure 3.14.

As it can be seen, the results obtained for any particular distance are slightly distributed at the initial period where the electric field strength under 400-V/cm. These are probably affected by the non-linear output of the HV generator system due to the presence of variac used for voltage control.



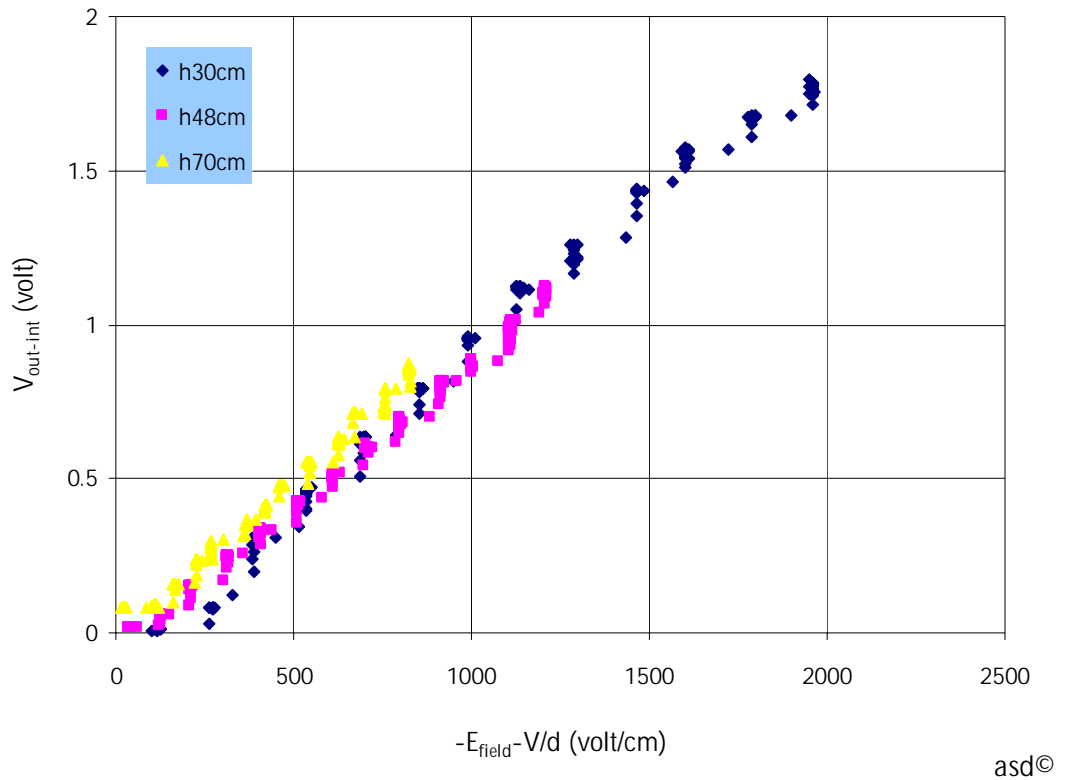


Figure 3.14 Simultaneous measurement results

The obtained results are analysed by using regression and correlation analysis to acquire empirical equation that can be used to present the relation between the electric field strength ( $E$ ) and the  $V_{out-int}$ . The empirical equation is the function between  $E$  with  $V_{out-int}$ . The relation can be written as:

$$V_{out-int} = f(E) \quad (1)$$

There are numerous mathematical model can be made base on above mathematical function. In this study, however, three mathematical models are studied to obtain the best empirical equation.

a. Linear:  $V_{out-int} = \alpha + \beta E$  (2)

b. Exponential:  $V_{out-int} = \alpha e^{\beta E}$  (3)

c. Power:  $V_{out-int} = \alpha E^{\beta}$  (4)

The  $\alpha$  and  $\beta$  are constants value that must be founded. The constants can be acquired by using least squares method.

Least square method is used to estimate the constant of linear equation as equation (2). However, it also can be applied to solve the equations (3) and (4) by modify the equations.

The equations (3) and (4) can be modified to the form of:

$$\hat{y} = \hat{\alpha} + \hat{\beta}x \quad (5)$$

Where,

$\hat{y}$  = dependent/response variable.

$\hat{\alpha}$  = intercept coefficient.

$\hat{\beta}$  = independent regression coefficient.

$x$  = independent/regressor variable.

a. Exponential:  $V_{out-int} = \alpha e^{\beta E}$

$$\ln(V_{out-int}) = \ln(\alpha) + \beta E \quad (6)$$

Where,

$$\hat{y} = \ln(V_{out-int})$$

$$\hat{\alpha} = \ln(\alpha)$$

$$\hat{\beta} = \beta$$

$$x = E$$

b. Power:  $V_{out-int} = \alpha E^{\beta}$

$$\log(V_{out-int}) = \log(\alpha) + \beta \log(E) \quad (7)$$

Where,

$$\hat{y} = \log(V_{out-int})$$

$$\hat{\alpha} = \log(\alpha)$$

$$\hat{\beta} = \beta$$

$$x = \log(E)$$

The least square estimates of the intercept and slope in the linear regression model are as follows:

$$\hat{\alpha} = \frac{\sum_{i=1}^n y_i}{n} - \hat{\beta} \frac{\sum_{i=1}^n x_i}{n} \quad (8)$$

$$\hat{\beta} = \frac{\sum_{i=1}^n y_i x_i - \frac{\left(\sum_{i=1}^n y_i\right)\left(\sum_{i=1}^n x_i\right)}{n}}{\sum_{i=1}^n x_i^2 - \frac{\left(\sum_{i=1}^n x_i\right)^2}{n}} \quad (9)$$

For calculating the correlation coefficient ( $r$ )

$$r_{xy} = \frac{\sum_{i=1}^n (y_i - \bar{y})(x_i - \bar{x})}{\sqrt{\sum_{i=1}^n (y_i - \bar{y})^2 \sum_{i=1}^n (x_i - \bar{x})^2}} \quad (10)$$

For calculating the multiple correlation coefficient ( $R^2$ )

$$R^2 = \frac{SS_R}{SS_T} = \frac{\sum_{i=1}^n (\hat{y}_i - \bar{y})^2}{\sum_{i=1}^n (y_i - \bar{y})^2} \quad (11)$$

Where,

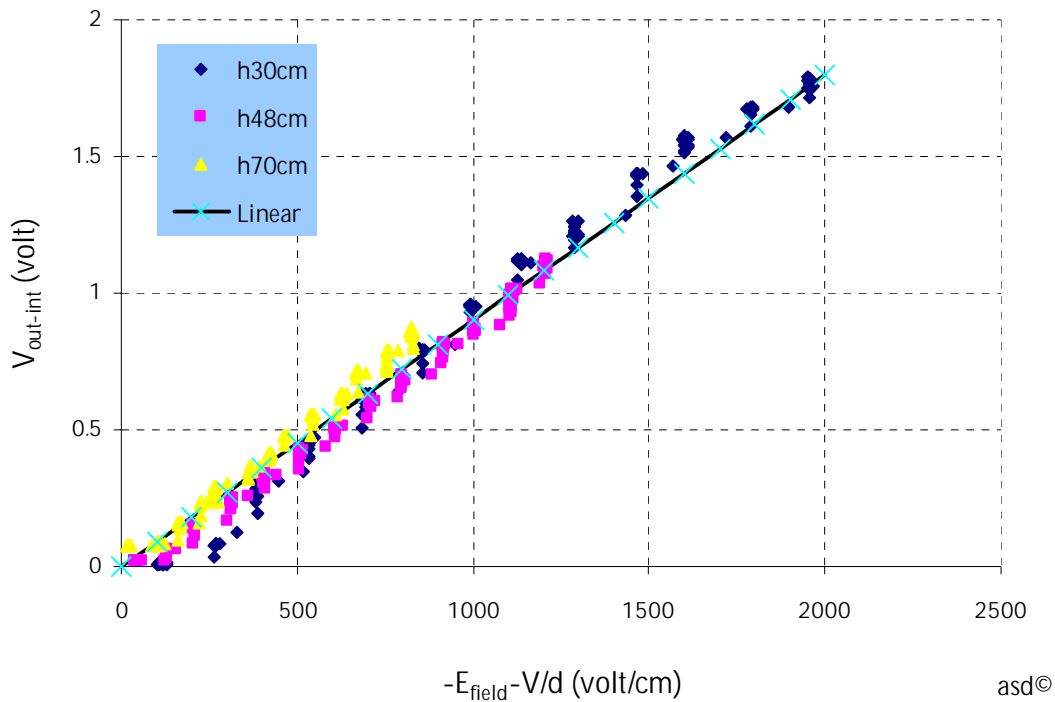
$SS_R$  = regression sum squares.

$SS_T$  = total corrected sum of squares.

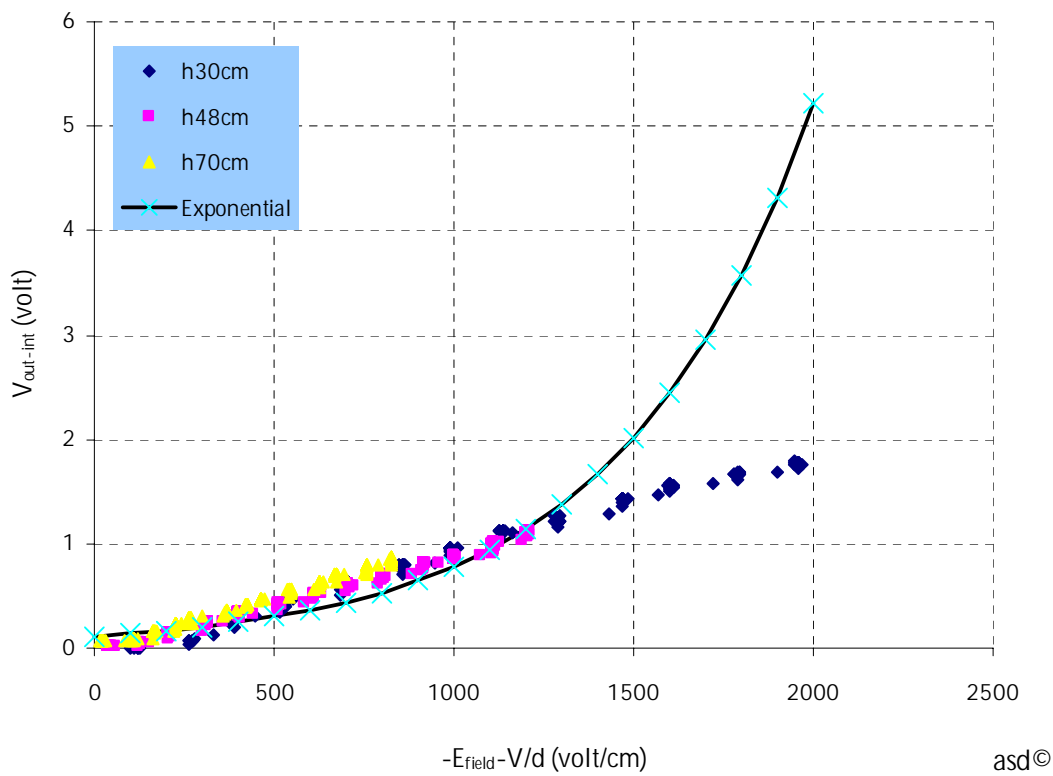
The calculation results are shown in Table 3.1 and Figure 3.14 gives the graph of mathematical equation models of simultaneous measurement results.

Table 3. 1 The constant calculation results and correlation coefficient

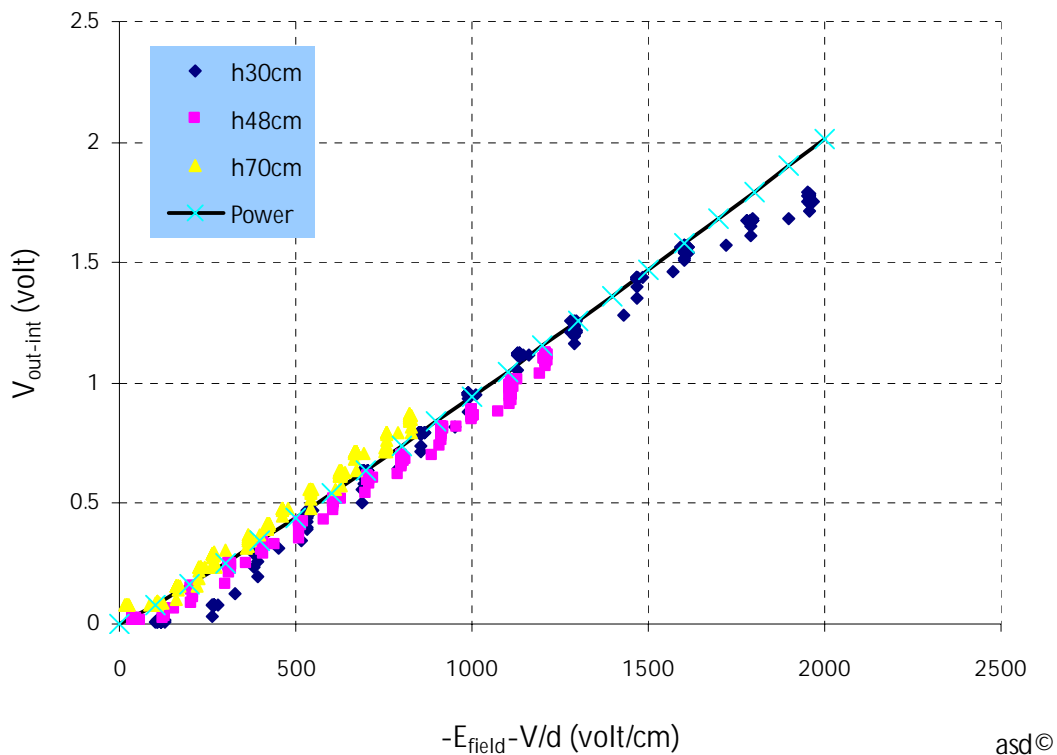
No	Mathematical Model	$a$	$b$	$r$ (correlation coefficient)	$R^2$ (multiple correlation coefficient)
a.	Linear	0	0.0009	0.9914	0.9828
b.	Exponential	0.1169	0.0019	0.8382	0.7025
c.	Power	0.0005	1.092	0.9213	0.8489



(a)



(b)



(c)

Figure 3.15 Mathematical equation models of simultaneous measurement results: (a) Linear, (b) Exponential, and (c) Power.

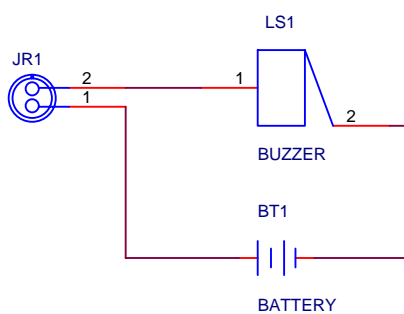
Based on the analysis it can be concluded that the linear mathematical model is the best model to present the correlation between  $V_{out-int}$  and  $E$ . Hence, the microcontroller is programmed as such to give a response based on calibration curve obtained previously.

### 3.6 Early Warning System and Laser Triggering System

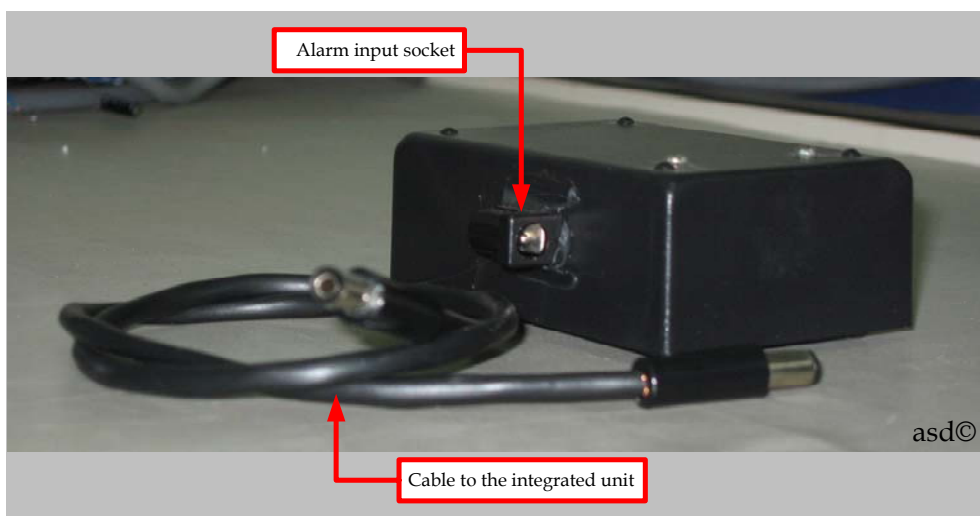
As described above the output signal from the relay is used to activate an early warning system and a laser beam triggering device in relation to specific electric field strength. The description regarding the early warning system and laser triggering are given in following subsections.

### 3.6.1 Early Warning System

The intention of the early warning system is to provide a precaution to individuals in the area of concern about there would be occurrence of lightning discharge to the ground. In this conjunction, a simple alarm unit using 1.5-V dry battery is developed as shown in Figure 3.16. However, other types of alarm system can be utilized for alarming system improvement.



(a)

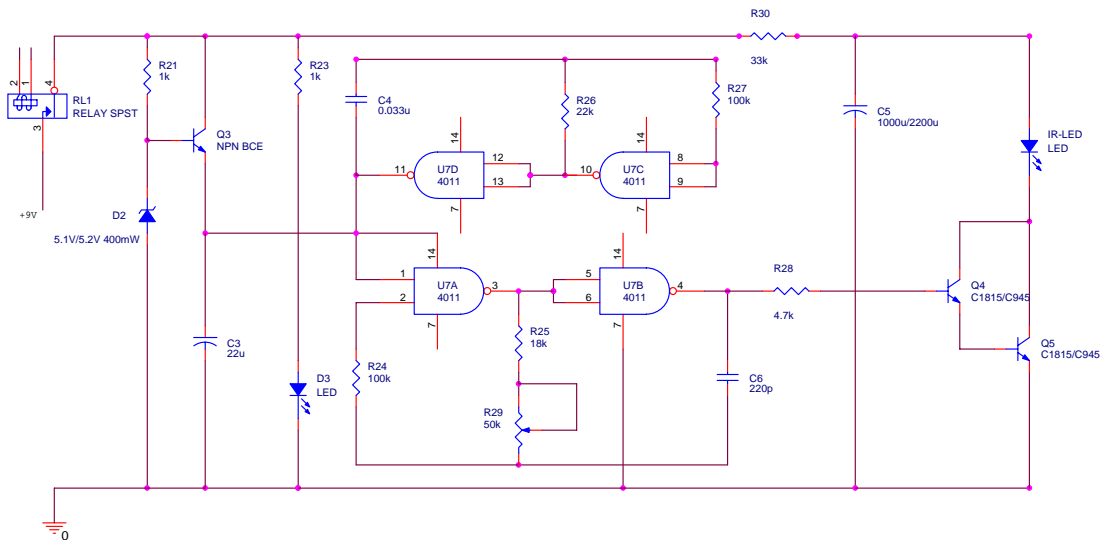


(b)

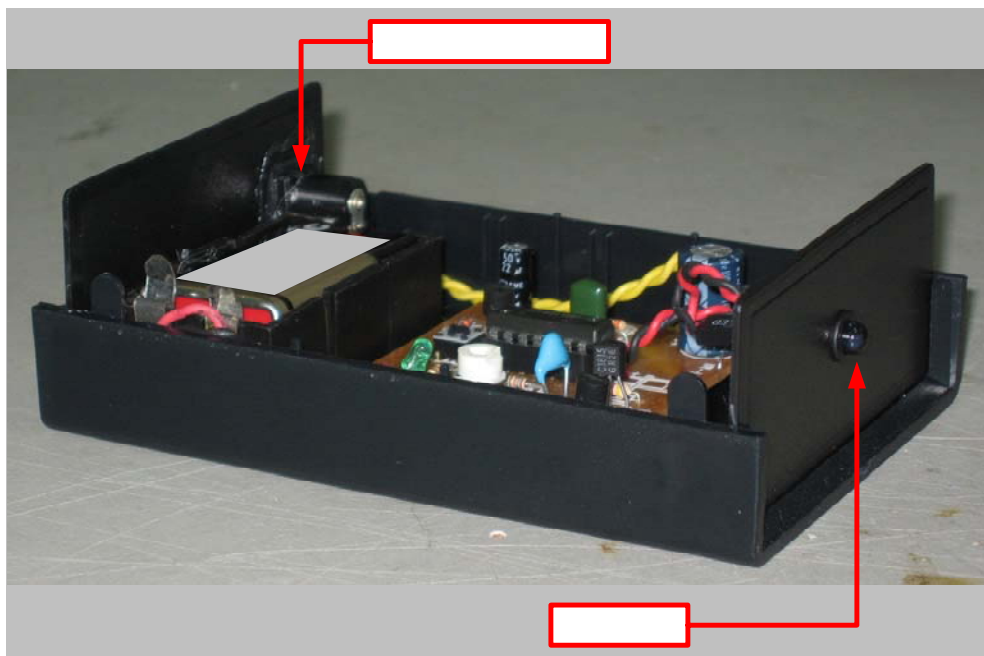
Figure 3.16 The mock-up of early warning system, (a) Schematic diagram and (b) The alarm unit with a cable length to the integrated unit

### 3.6.2 Laser triggering system

In order to activate the laser triggering systems, a remote infra red control unit linking to the integrated unit is developed as shown in Figure 3.17. This unit is supplied by a 9-V battery.



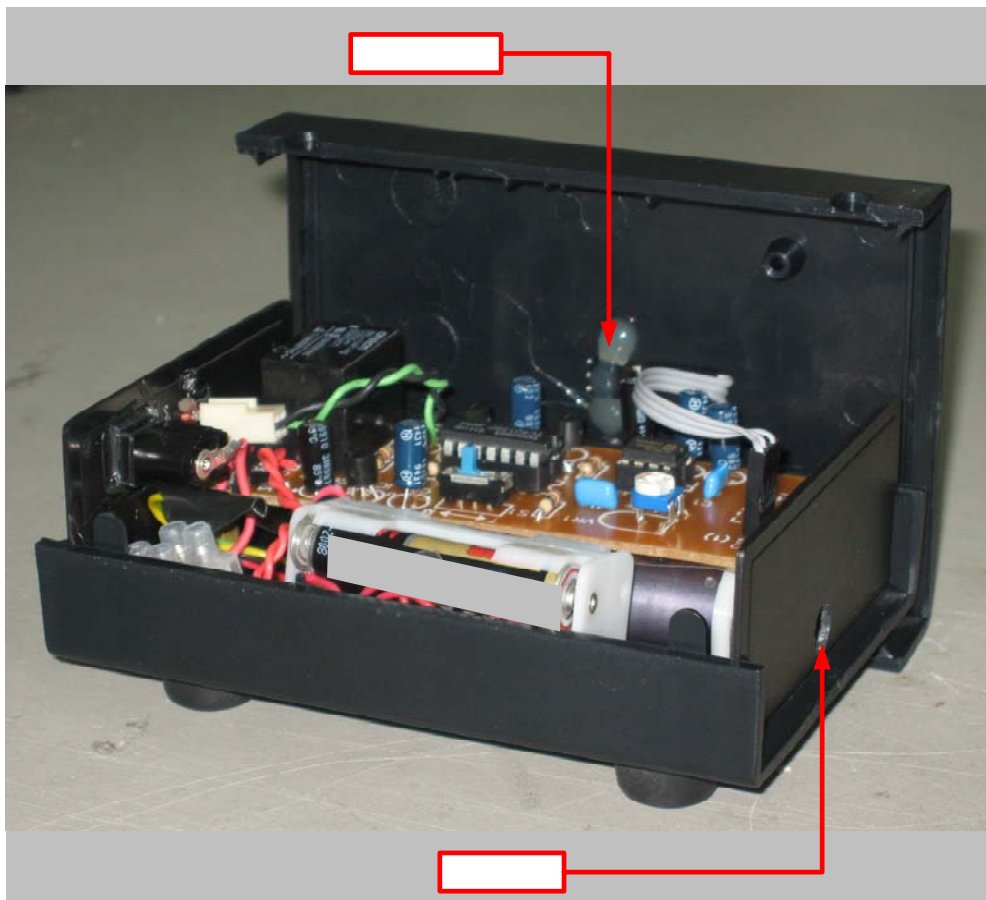
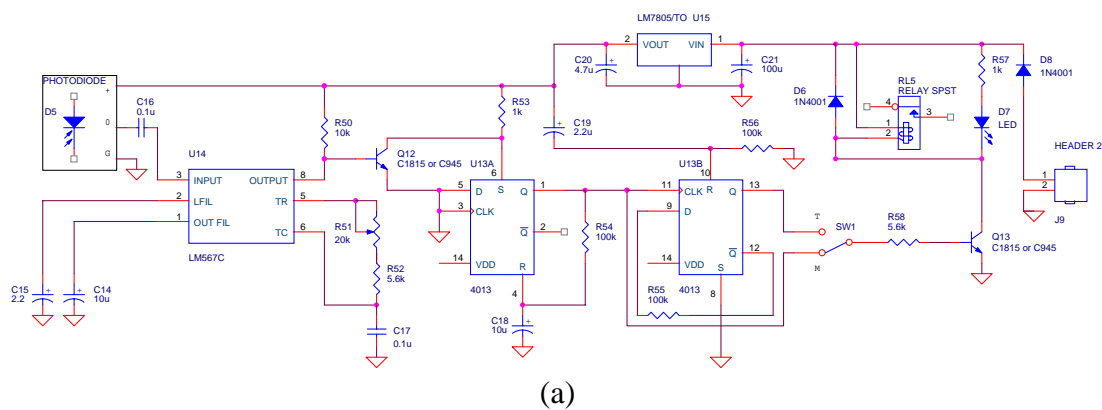
(a)



(b)

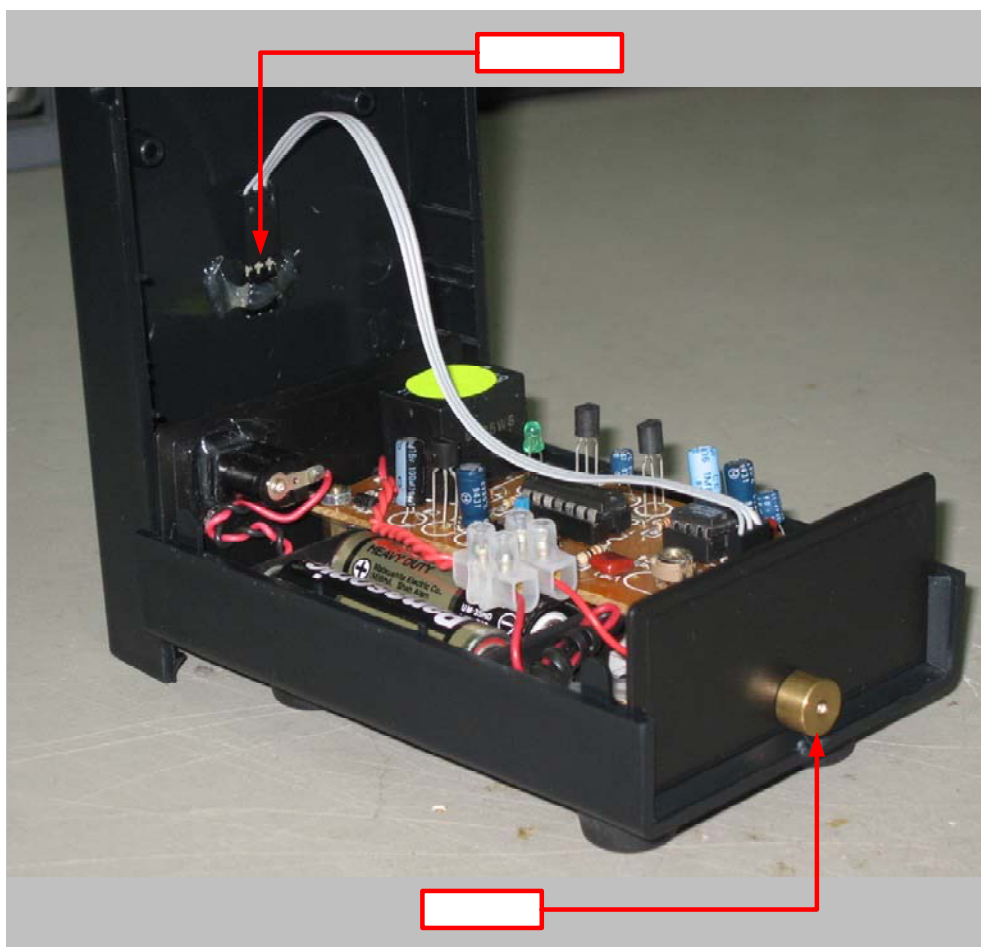
Figure 3.17 The infra-red remote control transmitter, (a) Transmitter schematic diagram and (b) remote infra red unit

There are two types of laser triggering system are developed in this present work. The different between them is the power rating of the laser trigger devices. Figure 3.18 shows the schematic diagram of infra-red receiver and the laser triggering units with power rate of  $\pm 20\text{-mW}$  and  $\pm 1.0\text{-mW}$  respectively.





(b)



(c)

Figure 3.18 The infra-red remote control receiver and the Laser system, (a) Receiver schematic diagram, (b) Laser triggering system  $\pm 20.0\text{-mW}$ , and (c) Laser triggering system  $\pm 1.0\text{-mW}$

### 3.7 A new concept of lightning protection system for strategic areas

The entire unit that have been described previous will be integrated to one sophisticate system. This novel concept is an idea in which a detection unit, a recording unit, blunt LAT(s), and a laser triggering unit are integrated to one system. The diagram of the LPS is presented in Figure 3.19. This work is initiated by developing a simulation and continued with developing of virtual measuring system.

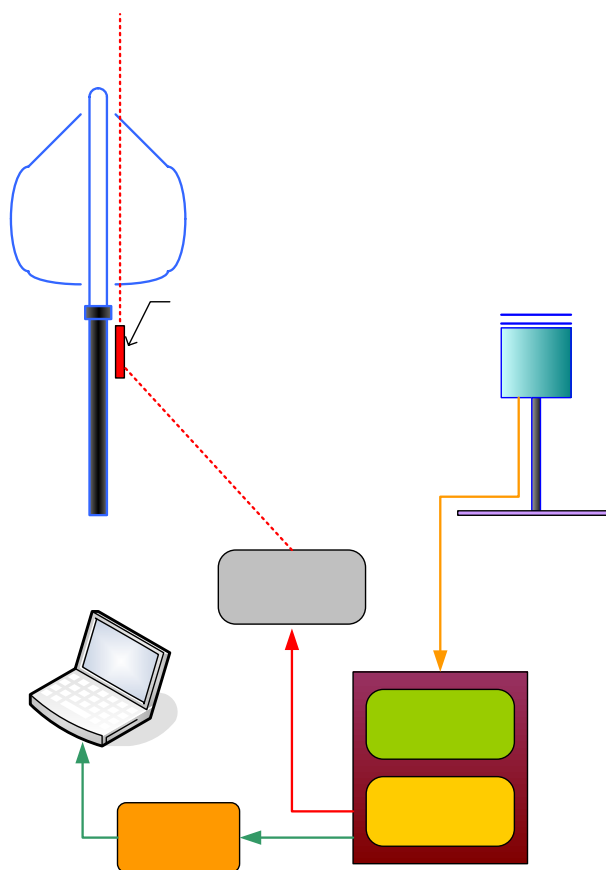


Figure 3.19 The diagram of the novel concept of LAT for strategic areas

Lightning ter

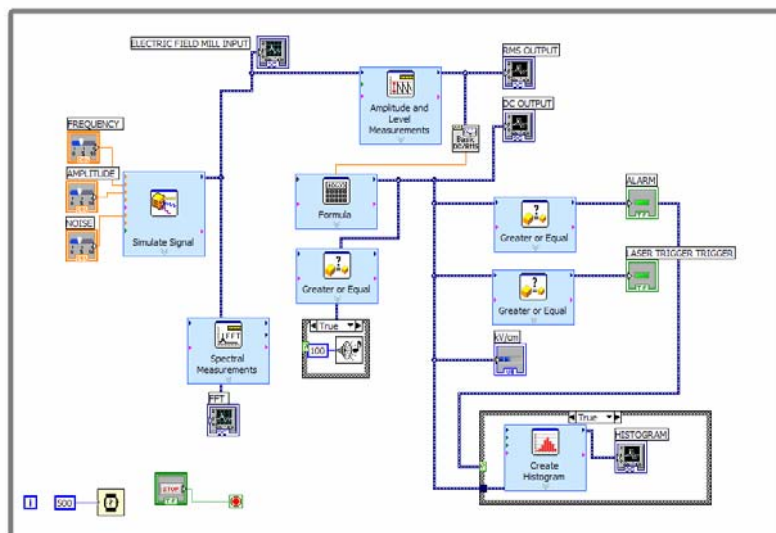
Laser t

### 3.7.1 Simulation of the new concept

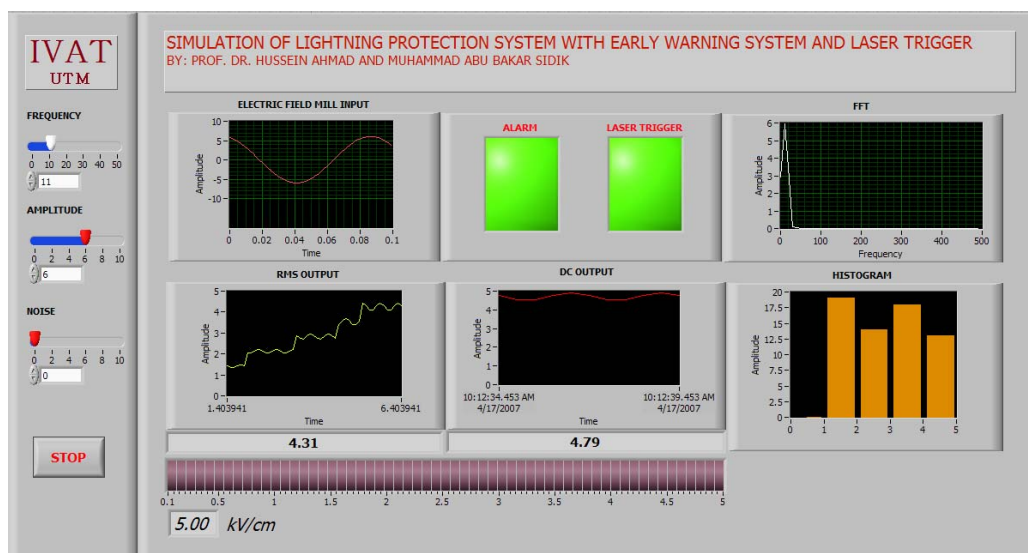
This subsection will present the simulation of the new concept. The simulation is developed by using LabVIEW. It consists of three main groups i.e. Input Block, Processing Block, Output Block. The detail of block components that are used for the simulation is shown in Table 3.2. Figure 3.20 shows the block diagram and the front panel of the simulation.

Table 3. 2 The simulation block components

1.	Input Block	Simulate Signal (Frequency, Amplitude, and Noise)
2.	Processing Block	Amplitude and Level Measurement Basic DC/RMS Formula Greater or Equal
3.	Output Block	Alarm Alarm LED Laser Trigger LED Spectral Measurements Create Histogram



(a)



(b)

Figure 3. 20 The simulation, (a) Block diagram and (b) Front panel

The Input Block is a virtual function generator of signals with noises (simulation) has been used to generate sinusoidal signal. The output signal of generator (input signal of spectral measurements) is connected to the FFT Spectrum block and presented in graph display. Computation of amplitude of the signal is made by using Amplitude and Level Measurement Block. Then the Basic Averaged DC-RMS block is used to compute the dc component and rms value.

Then the output is sent to a Formula block. This Formula block is used to place the equation that is acquired from subsection 3.5.2.

Setting parameters of analyzed signal (amplitude, frequency, noise level) can be performed at the front panel. When the output of the Formula block is higher than 1-kV/cm the computer alarm will be turn-on and also the alarm LED display. If the output increases continually until it attains 2-kV/cm then the Laser Trigger LED will be turn-on.

This simulation displays also a Histogram graph. Where the axis  $x$  describes measurement scale of acquired results of ambient electric field strength and draw the boundaries. The  $y$  axis presents value of frequency distribution which describes how often such result happened. The histogram provides visual impression of the shape of the distribution of the measurements as well as information about the scatter or dispersion of the data [68]. By analyzing the histogram the information regarding to which value revealed most often can be obtained.

### **3.7.2 Computer Measuring System**

A measuring system can consist of measuring devices linked through interface to a computer. This combination is recognised as Computer Measuring Systems (CMS). By using CMS, set of tools, methods, and operations (hardware and software) are designed to realize the operation which is necessary to perform measurements [65-67]. Mostly the operations consist of setting of excitations, collecting measured data, processing data, and saving or transmitting data.

Generally CMS apply the graphical interface named Human Machine Interface (HMI) as the communicator between the computer and the operator [63,64]. The display of computer's monitor can be presented similar to those used in real instruments; therefore it is named virtual measurements instrument. Every parameter can be changed by using virtual switches, virtual sliders, and knobs. Currently a number of measuring softwares are applied for creating virtual measuring instruments (VMI); there are LabVIEW, VEE-Pro, Test Point, DasyLab, Lab Windows, and MATLAB Data Acquisition Toolbox [66,71].

The development of the VMIs can be distinguished into two types [71]. Firstly it is built on the basis of the data acquisition board (DAQ) where practically all the measuring procedure is made by the computer. Secondly it can be created by standard measuring devices, for instance multimeters or generators linked to the computer through interfaces. In the latter the measuring instruments operate as a tool of the computer virtual instrument.

The virtual measuring instrument of EFM of Early Warning System and Laser Trigger (EWarS&Laser) is developed on the platform of LabVIEW for monitoring and recording the ambient electric field condition.

The data acquisition (DAQ) that is used to collect the signal from the Integrated Unit is a PicoScope 3026 from Picotech. The working principle of the PicoScope is similar with an oscilloscope however it is designed to be applied with virtual measuring instrument. This PicoScope is accompanied with USB 2.0 interface to communicate with computer so that the data transfer can reach 480-Mbps [69,70].

The input signal is received from the Integrated Unit. When the Integrated Unit activate the early warning system and laser triggering unit, the software simultaneously turns on in the computer alarm and LED. The other displays are presented similar with the simulation module in subsection 3.7.1. Figure 3.21 presents the VMI of EWarS&Laser version 1.05. However, the detail block diagram is given in the appendix.

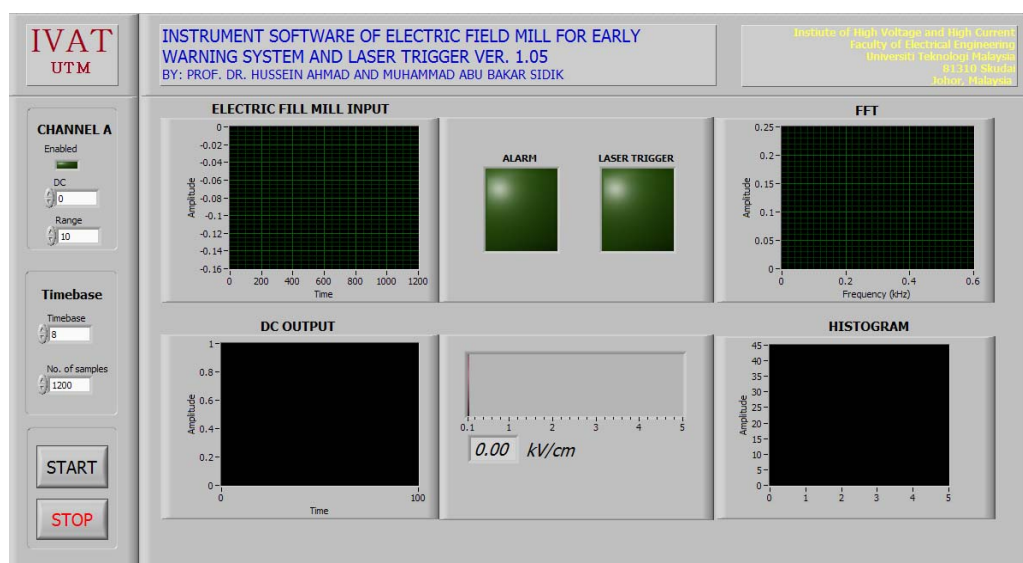


Figure 3.21 Front Panel of VMI of the EWarS&Laser version 1.05

## CHAPTER 4

### Development A New Direct Strike Lightning Air Terminal Using Electrostatic Generator Concept

#### 4.1 Introduction

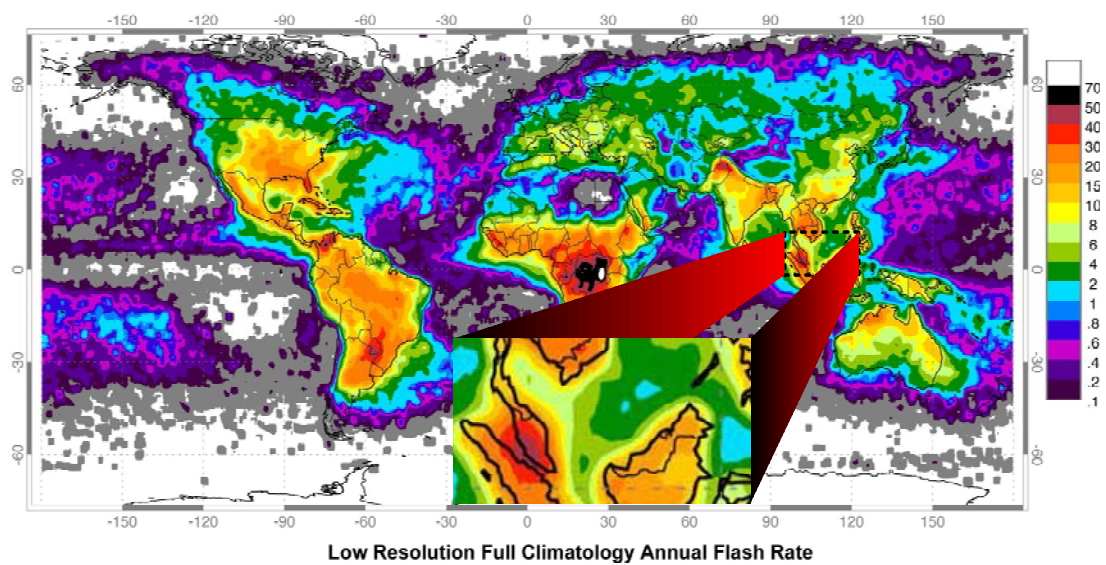
Lightning intensity in Malaysia is very excessive. This due to Malaysia locates near the equator (latitude  $1^{\circ}$ - $7^{\circ}$  N and longitude  $100^{\circ}$ - $119^{\circ}$  E). However, Malaysia's climate somewhat differs from that of other equatorial areas due to it is experienced to the monsoonal winds. The maritime condition contributes an important role in formation of climate in Malaysia as well as the interchange of wind systems from the Indian Ocean and the South China Sea [72]. Figure 4.1 depicts the Malaysia map.



Figure 4. 1 Malaysia location in the globe [73].

The Malaysia Peninsular and the State of Sabah and Sarawak in the north western coastal area of Borneo Island occupy an area about 330, 307.1-km<sup>2</sup> [72]. Highest temperature recorded is 40.1°C recorded at Chuping Perlis on 9 April 1998. Lowest temperature recorded is 7.8°C recorded at Cameron Highlands at altitude 1471.6m above Mean Sea Level on 1st. February 1978. Highest mean daily wind speed is 3.1 m/s recorded at Mersing, Johor. Highest maximum wind speed is 41.7 m/s recorded at Kuching, Sarawak on 15 September 1992 [75].

Malaysia's hydro-meteorological parameters present the most favourable condition for thunderstorm activity. Highest mean annual numbers of days with lightning is 317 days recorded at Subang. The analysis was based on 50 years (1951 to 2000) records of 36 principle meteorological stations [75]. The thunderstorm activity around the globe according to NASA is illustrated in Figure 4.2



Global distribution of lightning April 1995-February 2003 from the combined observations of the NASA OTD (4/95-3/00) and LIS (1/98-2/03) instruments.

Figure 4. 2 Lightning Map the black area in Central Africa is where the greatest lightning activity occurs. Reds, oranges and yellows are areas of high activity while areas in white or blue have low activity [74].



As given it is clear that lightning intensity in Malaysia will be an extraordinary problem for their people, especially when they develop into more modern industrialized and increasing in population.

In order to minimize the catastrophic effects of the lightning strike, LPSs are necessary. Properly LPSs consist of three basic elements: lightning air terminal (LAT) units, down conductor units, and grounding system units. The function of LAT is to intercept lightning leaders around certain area of zone protection and pass the lightning current to the grounding system through the down conductor(s). Banking on the methods of the conventional LAT is with consequences. Many buildings are damages though the LAT are installed. The current existing LATs being used do not always ensure the desired level of efficiency where there are still problems of protection of terrestrial object against lightning.

With increasing height of structure for instance telecommunication tower or modern multi-storeys buildings lightning strike will possibly invoke serious damage to the related equipments. According the investigation upon numerous building in Kuala Lumpur, Malaysia installed with conventional LAT it is found that struck point disperse to a particular place around instead of the conventional LAT [34]. Therefore an effort to improve or to discover a new way to intercept lightning downwards leaders is necessary.

In order to emerging with a better solution, a new direct strike (DS) LAT has been developed. The improvement is made base on the original design of blunt rod LAT and then incorporated with obvious concepts of electrostatic generator and laser beam.

The computer modelling of the new DS LAT's is made by using CAD drawing tools software. The computer modelling contributes an important role to describe the geometries shape. Therefore it is a necessary stage before a physical modelling is developed. From the computer modelling, the appearance of the product can be presented identically to the real object. Moreover in some studies computer simulation and analysis works can be performed on the model.

However computer model cannot provide a realistic illustration of the actual size DS LAT. For that concern a physical model is necessary to be developed. The physical model could be made by using some varieties of materials, for instance papers, styrofoams, woods, and others which are cheap and easy for customisation.

Prior to manufacture of the First prototype the material specifications are determined. The selection of material is considered on the basis of their performance in outdoor circumstance. The First prototype performance and geometries shape will be evaluated and then a laboratory testing will be made to see its performance. Observation results that are made on the First prototype will be used to formulate several necessary improvements for the Second prototype. After final evaluation on Second prototype a new detail drawing set will be produced. The flow chart of the approach to develop the LAT is given in Figure 4.3.

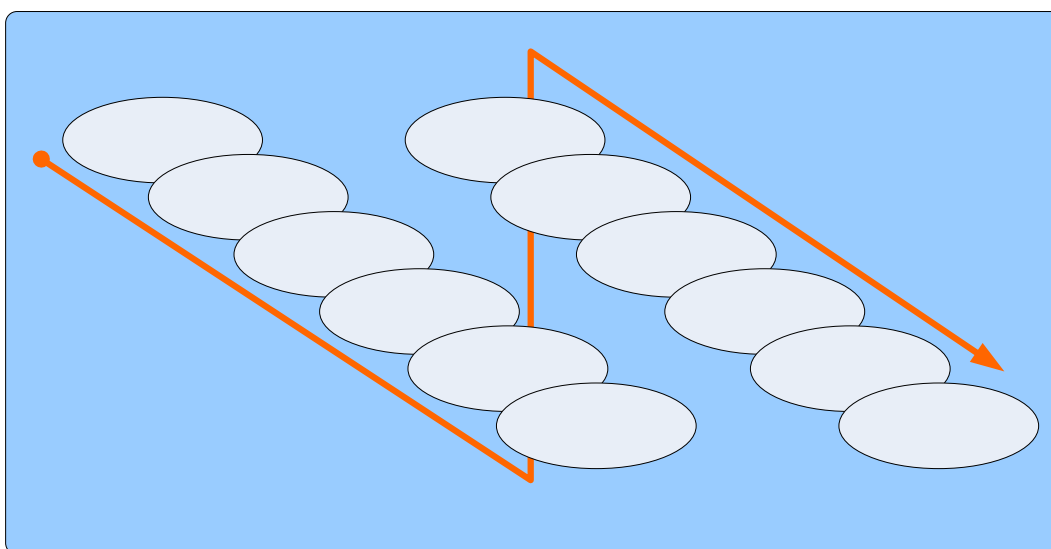


Figure 4. 3 Process flow of LAT prototype development.

## 4.2 Objective

The main objective of this study is to <sup>Recognized the need</sup> come-out with a new DS LAT which is looked into LAT which can produce numerous competitive upward streamers from the LAT to affect higher probability of lightning leaders <sup>Original design</sup> being captured by the LAT.

Conceptual design

Computer modelli

Phy

Man  
p

### **4.3 Scope of work**

There are several methods that have been introduced to test the performance of LATs. The most accepted method is to place the LAT in the natural lightning, which is sometimes involves a rocket trigger lightning system. This testing is very costly because it requires a large research area with all its facilities. Currently the testing is only available in other countries. Therefore this prototype will only be tested in IVAT by using a 2.0-MV impulse generator. The natural lightning testing is planned to be performed in the future.

Also the laser system of the new DS LAT will not be activated since the performance of laser to attract lightning downward leaders has been proved by many authors as described in Chapter 1.

### **4.4 Research Methodology**

This section gives the explanation of the conceptual design of generating electrostatic field, the computer modelling, and the new DS LAT prototypes.

#### **4.4.1 Conceptual design**

This new DS LAT is a combination of several elements observed from the literature study in Chapter 1 could improve the performance of LAT. Those are blunt rod tip, free charges, and laser. In order to accommodate all the elements above the new DS LAT is separated into three main units: static unit, a laser triggering unit, and a rotating unit.

The static unit consists of blunt rod tips, two field plates as capacitor, and conductive brushes. The diameter of blunt rod is about 19-mm which is based on C.B. Moore's study at which the blunt rod in that size have intercepted more lightning downward leaders than others.

Free charges are produced by using the electrostatic generator. There are many types of electrostatic generators. With a peer review, it is determined that the most appropriate concept for this DS LAT is the Varley machine concept. The model of the Varley machine is shown in Figure 4.4.

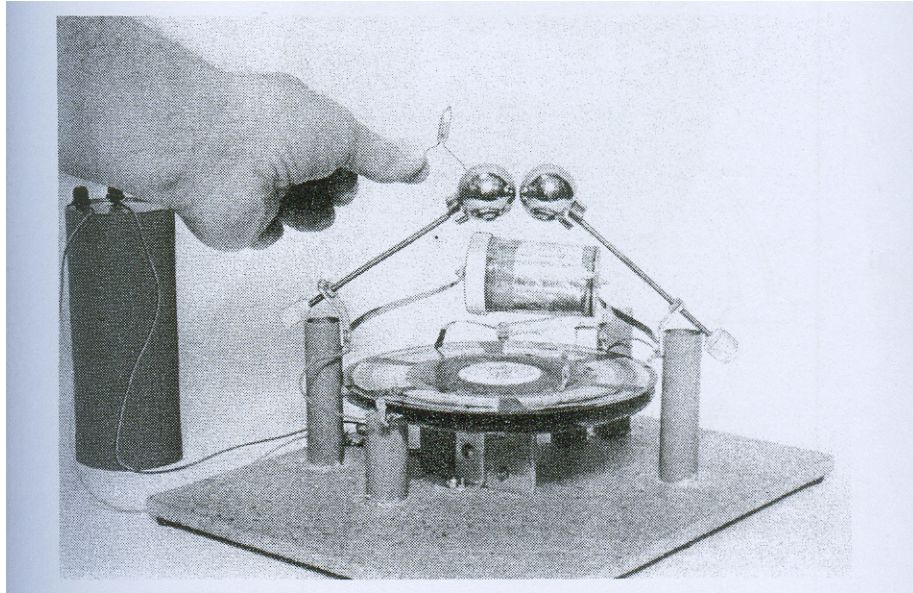


Figure 4.4 Varley machine [76].

Base on the Varley machine concept, an innovation has been made to produce an electrostatic generator, which can be applied for this new DS LAT. The electrostatic generator model is developed consists of 2 (two) cylindrical tubes. The schematic diagram of the model is given in Figure 4.5 and Figure 4.6 presents the electrostatic generator model.

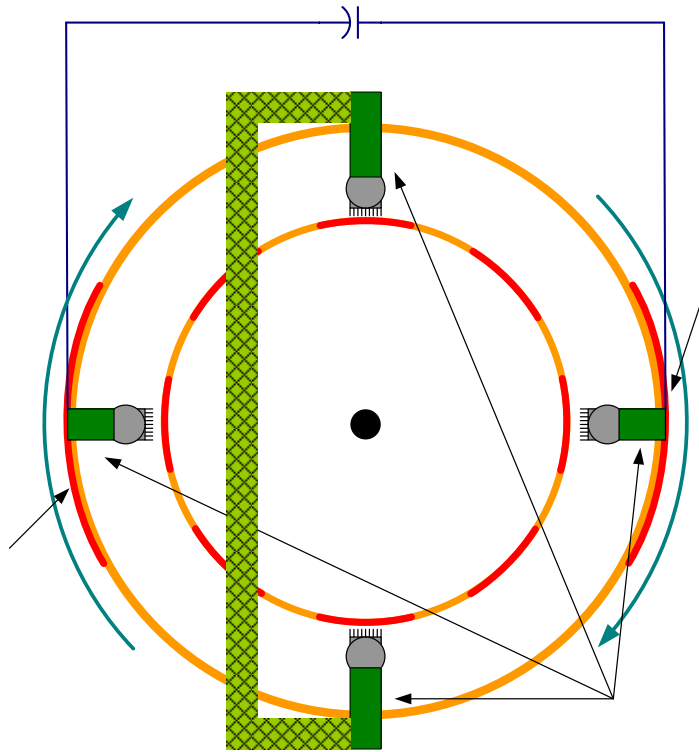
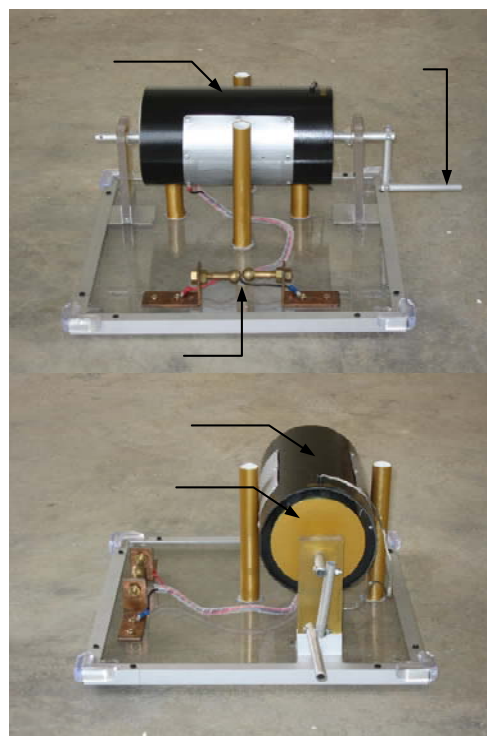


Figure 4. 5 Schematic diagram of electrostatic generator model.

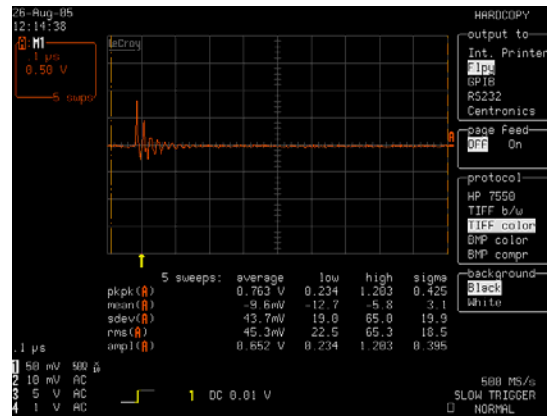


tation

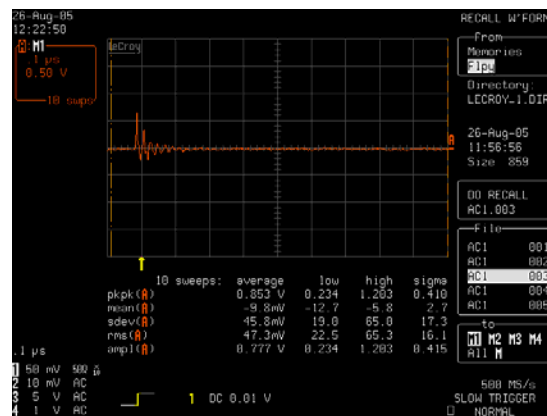
Figure 4. 6 Electrostatic generator model.

Presume that the initial charge on the field plates is zero. When the inner tube is moved, by rotate the hand cranks, the movement of the air through the field plates initiates a small electrical charge to arise on each plate. In this condition the each plate will possess dissimilar electrical charges; one plate is positive the other plate is negative. Since the rotation aluminium segment moves through the field plate, by induction an electrical charge will be developed in the segments. In every period of rotation two metals segments is connected by the set of fixed brushes, between them there will be a flow of surplus electron. As a result there will be different polarity between two aluminium segments, one is charged positively and the other is charged negatively. Afterwards every of the segments will be charged by induction to the polarity opposite that of its field plate. The rotation of the disc will then bring each charged field plate to a field plate brush, and the electric charge will then be transmitted through the brush to its field plate. This process repeats with each of the other metal segments for each rotation, increasing the electrical charge on the field plates. As the electrical charges increase on the field plates, the induced electrical charges of the rotating foil segments will also increase. Therefore, in a short time, the electrical charges will rise to a very high voltage. The capacitor is connected, between the field plates. When then capacitor is charged up to a high voltage, it will discharge through its internal spark gap and across to grounded rod. The rotation of the disc then repeats the whole process of induction; charging the field plates and capacitor until electrical energy is accumulated at a voltage high enough to discharge through the spark gaps. The spacing of the metal balls determines the rate at which the charging and discharging take place [76].

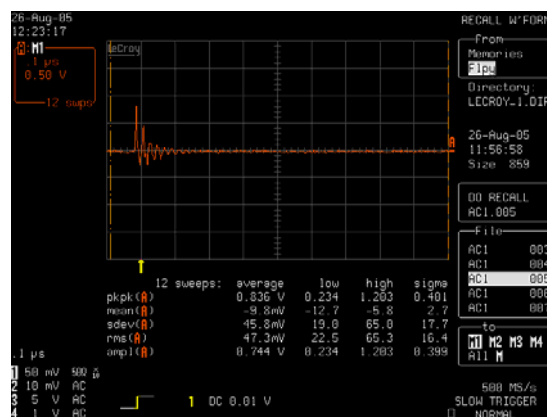
In field application wind energy is utilised to drive the rotating unit of the new DS LAT. When the wind blows in a particular degree of velocity, the rotating unit of the DS LAT will move. Figure 4.7 shows the obtained outputs of the electrostatic generator model.



(a)



(b)



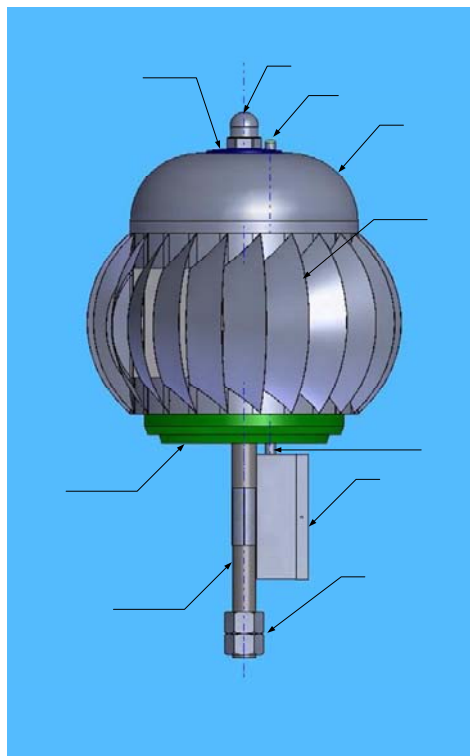
(c)

Figure 4. 7 Numerous outputs of electrostatic generator model.

#### 4.4.2 Computer modelling

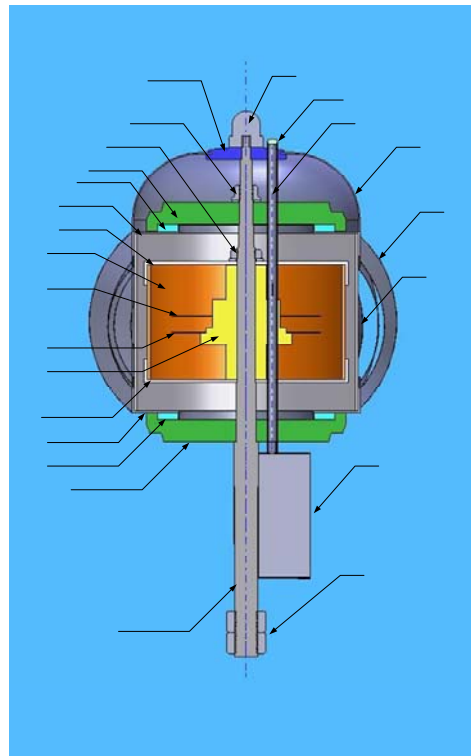
The computer modelling is initiated by a series of model design sketches. From those, a computer model was made by using Solidworks 3D Mechanical Design and 3D computer-aided design (CAD) software as a design tool. Solidworks is new generation 3D solid modelling software. It is a flexible and easy to use design tool; Its application is used widely in many engineering field.

By using Solid work, firstly each component is drawn separately and next they are combined altogether. There are twenty four components of the new DS LAT is modelled. Figure 4.8 shows the new DS LAT computer model. The dimension of the LAT is roughly 250-cm (diameter) and 240-cm height. The detail drawing design is provided in appendix.



(a)





(b)

1. Blunt tips, 2. jointer, 3. nut, 4. nut, 5. nut, 6. shaft, 7. top bearing holder, 8. top bearing, 9. outer tube top cover, 10. bottom bearing holder, 11. bottom bearing, 12. outer tube bottom cover, 13. outer tube, 14. leafs, 15. inner tube top cover, 16. inner tube bottom cover, 17. inner tube, 18. disk support, 19. bottom disk, 20. top disk, 21. dome, 22. laser box, 23. laser channel, 24. laser channel cover.

2  
3  
4  
8  
7  
9  
15  
17  
20  
19  
18  
16  
12  
11  
10

Figure 4. 8 Computer model of DS LAT, (a) Full model and (b) Section view of the new DS LAT.

Different from the former model of electrostatic generator where the moving part is the inner tube, in the new DS LAT the moving part is the outer tube. Figure 4.9 shows the schematic diagram of electrostatic that applied to the new DS LAT.

On the inner tube two field plates are embedded at which for every plates a conductive brush is attached as well a capacitor. For the outer tube, segmentation is made by using aluminium sheets.

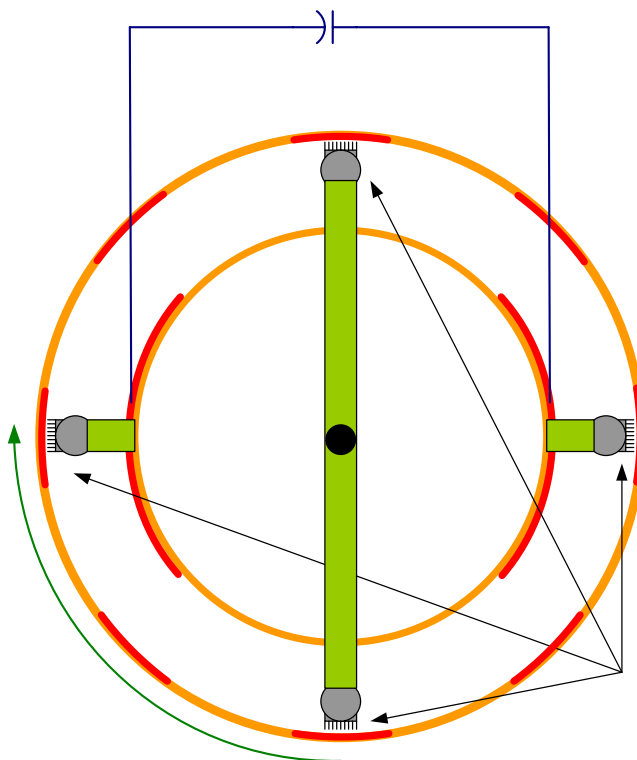


Figure 4. 9 Diagram of electrostatic generator applied on DS LAT.

#### 4.4.3 Development the Prototype

Field plate

There are two prototypes have been developed after the computer modelling completed. Generally the new DS LAT has 3 basic constructions. The central supporting is the lightning rod grounded. Secondly a wind-powered rotating turbine (WPRT) encircled the rod. Thirdly a capacitor, charges as WPRT rotates. The capacitor energizes the floating hemispherical metal cap to high voltage. Due to this, ionisation of air occurs at this blunt tip of rod. Combining the dimensional size, rotating blade and ionisation of air, makes the product more efficient lightning captor. Figure 4.10 shows the two prototypes.

Rotation



(a)



(b)

Figure 4. 10 New direct strike lightning air terminal, (a) first prototype, and (b) second prototype.

#### 4.5 Experimental Setup

To observe the performance of the new DS LAT numerous tests has been made in Institut Voltan dan Arus Tinggi (IVAT), Faculty of Electrical Engineering, Universiti Teknologi Malaysia by utilising up to 2.0-MV impulse voltage (1.2/50- $\mu$ s) of 20 stages Marx generator.

There are two competitive tests were made to observe the performance of the new DS LAT. It comprises three main components, the HV generator, a sharp rod electrode (SRE) and a digital camera. The general setup is depicted in Figure 4.11

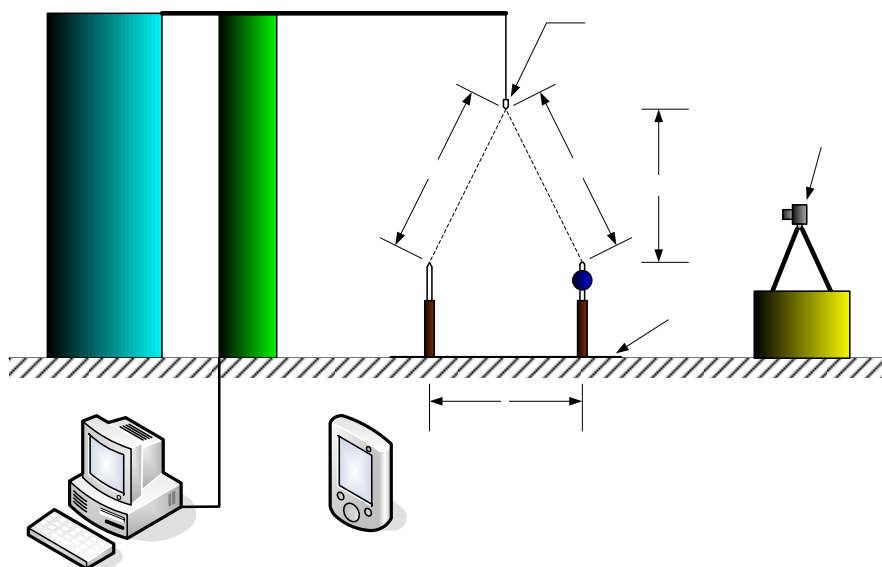


Figure 4. 11 General setup of the competitive testing.

The competitive tests were conducted under similar electrogeometrical condition where the SRE was located above the LATs. There are two distance setting applied in these experiments: for the first prototype the distance ( $d$ ) is set to 0.5-m and for the second prototype the height ( $h$ ) is set to 1.0-m. In these experiments there is no special purpose regarding “ $d$ ” or “ $h$ ” setting it is merely to differentiate the distance.

For the span ( $s$ ) between two LATs set to 1.0-m. Since the laboratory free area is very limited, a larger of “ $s$ ” than 1.0-m is possibly ineligible to be performed.

20 stages Marx Generator

HV Impulse Divider

Figure 4.12 shows the distance setting of the first prototype meanwhile for the second prototype is given in Figure 4.13.

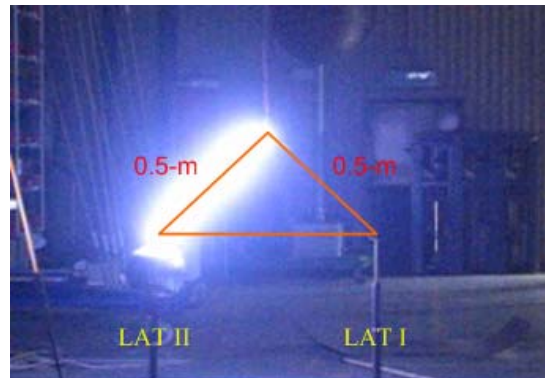


Figure 4. 12 Testing setup for First prototype, showing the distance of the competitive test.

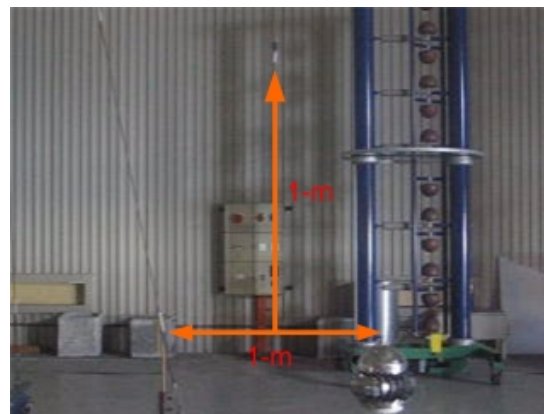
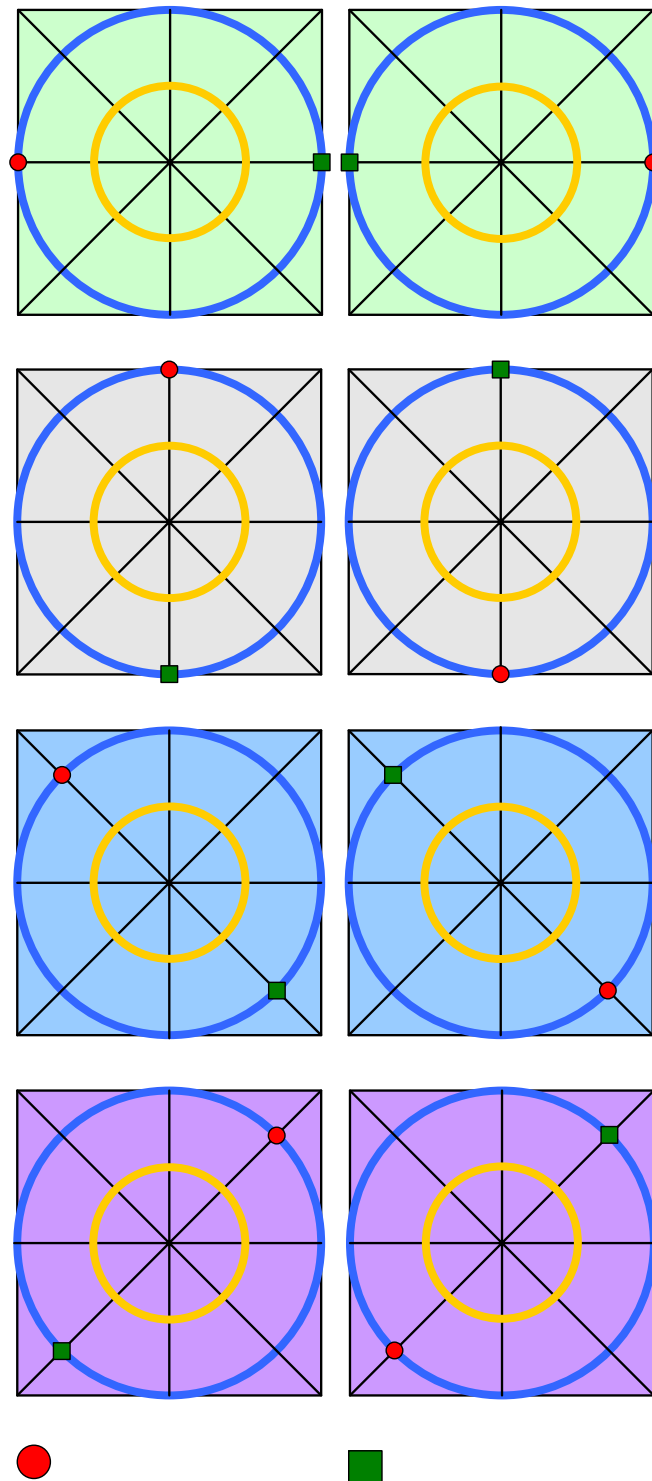


Figure 4. 13 Testing setup for Second prototype, showing the distance of the competitive test.

The tested LAT samples positions were rotated at  $45^\circ$  and swapped over to interchange their positions as shown in Figure 4.14 to eliminate errors in the testing results mainly due to impulse electrostatic field distribution irregularity.

Five times negative impulse is applied to the rod electrode for every LAT positions during the experiments. The voltage applied to the SRE is observed by using DIAS system through the voltage divider. In order to avoid inaccurate results these experiments were made under almost similar atmospheric condition for every discharge occurrences. The occurrence numbers of discharges were measured when

lightning impulse voltage was applied to two LATs simultaneously. The light emitted during the discharge is captured with a 7.1-mp digital camera.



A

Figure 4. 14 Tested LAT samples positions

C

## 4.6 Results and Discussion

The early finding found that by applying total shots of 40, 800 kV of lightning impulse voltage to the LAT I and LAT II obtained only 13 shots hit the former. Figure 4.15 present the detail of the First prototype competitive testing result. Further on the Second prototype testing, it was found that from the total shots of 40 acquired only 15 shots hit the LAT I as illustrated in Figure 4.16. Details of testing results included the atmospheric condition is given in appendix.

Figure 4.17 show a result of lightning impulse discharge (LID) of the competitive test of the First prototype and Figure 4.18 depict a result of the competitive test of the Second prototype. Interestingly an upward streamer developed on the LAT I captured also in this competitive testing as highlighted in the circle of the Figure 4.15 and also obtained that the lightning impulse discharge (LID) on the new DS LAT was not always hit the LAT tips; in several occasions the LID hit the “leafs” of the LAT. This is shown that geometrical form of LAT probably has a large contribution for intercept the LID.

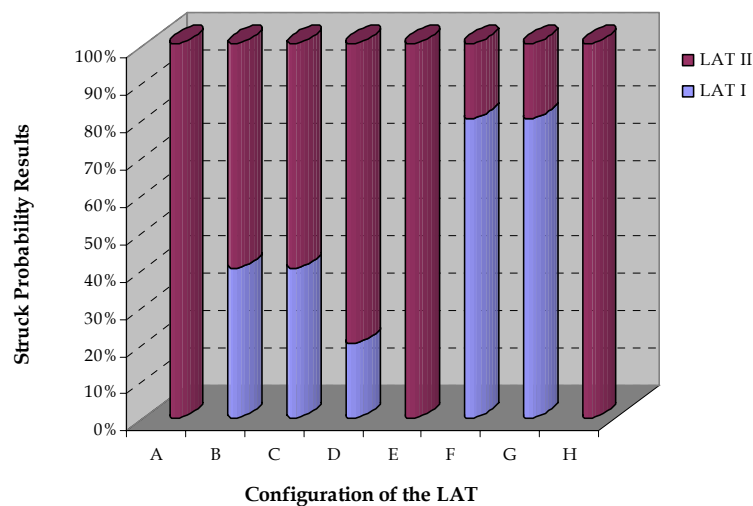


Figure 4. 15 First prototype testing results.

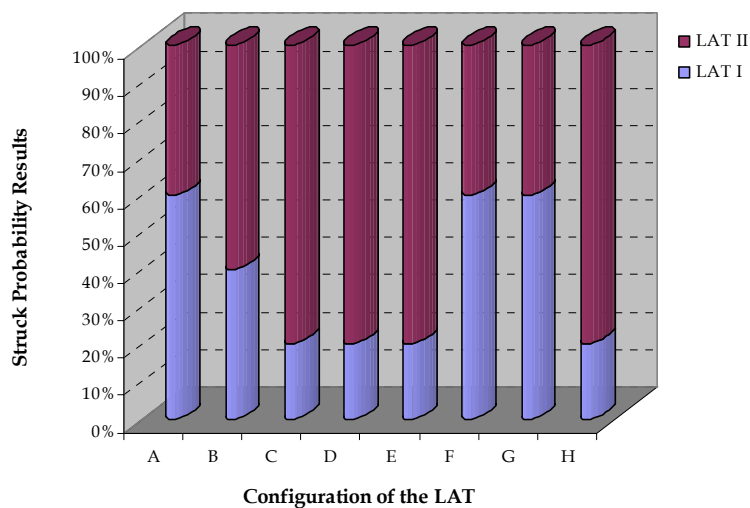


Figure 4. 16 Second prototype testing results.



Figure 4. 17 A result of lightning impulse discharge of the competitive test for the first prototype where the upward streamer was also developed on the tips of the conventional LAT.



Figure 4. 18 A result of lightning impulse discharge of the competitive test for the second prototype.



## 4.7 Conclusions

This early laboratory testing has provided a good figure concerning the performance of the new LAT. However further testing has still to be made in different distance of electrode with the LAT. Field observations is also necessary to be carried out.

The LPS standards guide are a very good accomplishment and a necessity in providing guidance to avoid destructive effects of lightning strikes. Therefore any improved method is acceptable as a standard practice or not makes future developments of LAT more exciting and challenging. Research and development efforts are important scientifically acceptable to lightning scientists and engineers.

From this observation it can be concluded that geometrical shape has an importance effect to intercept lightning leaders. Moreover, the testing of LAT in laboratory has to consider the impulse electrostatic field distribution irregularity therefore it is very importance to interchange the position of lightning air terminal subjected in the competitive testing.

## **CHAPTER 5**

### **General Conclusions and Future Works**

#### **5.1 General Conclusions**

A series of efforts have been made to provide a new knowledge and technology regarding LPSs. The effort is initiated by made experiments and analysis regarding the corona discharge formation and current on the various tips of known as conventional LAT. It is found that tip areas that form sharp edges provide important role in formation of corona. Obviously the corona formations influence performance of LAT since the corona development act like a shielding. Thus damaged LAT which develops more corona current possibly has lowest probability to intercept lightning downward leaders. This is inline with the results that acquired by Moore. CB.

A new application of the Dimensional Analysis is also provided to analyse the corona current. From this an equation with a new constant is introduced on the basis of experimental results.

In the second stages these current works look into the development of indigenous EFM for early warning systems and laser triggering. Almost the whole process for developing the sophisticate system is conducted in Laboratory of Institut Voltan dan Arus Tinggn (IVAT). This development initiated from zero.

Firstly Peer review is made regarding the existing EMF and its application. It is found that this work invoke a new idea to applying laser triggering lightning by using infra-red controller technology.

The last stage is development of a new DS LAT by combining three components that possibly increase the probability to intercept lightning downward leaders. Two prototypes have been developed which is initiated from sketches to computer modelling. Even with limited facilities for performance LAT test, numerous laboratory tests is conducted in IVAT. The consideration is if the new DS LAT shows a good performance with this kind of laboratory testing then further step will be conducted. In this kind of laboratory testing a new method is introduced; it is by rotated at  $45^\circ$  and swapped over to interchange their positions of the tested LAT samples positions to eliminate errors in the testing results mainly due to impulse electrostatic field distribution irregularity. The laboratory testing provided good figure regarding the performance of the new DS LAT.

## **5.2 Future Works**

This current works has opened many opportunity for further researchs.

1. The corona discharge current of various types of conventional LATs possibly to be proceeded to automatic detection of LAT tips formation.
2. The early warning system has potential market especially in Malaysia where Malaysia's product does still not found in the market. However field applications are not conducted yet.
3. The laser triggering with infra-red controller technology and also the new DS LAT can be continued with field testing.

## REFERENCES

1. V.V. Appolonov, L.M. Vailyak, I.P. Vereshchagin, V.V. Glazkov, D.N. Gerasimov, I.G. Kononov, A.V. Orlov, D.N. Polyakov, O.A. Sinkevich, M.V. Sokolova, A.G. Temnikov, K.N. Firsov, (2002), “Experimental Simulation of a Laser Lightning-Protection System on a Device with an Artificial Cloud of Charged Aqueous Aerosol”, *Journal of Quantum Electronic*, pp. 523-527, 2002.
2. Pater Hasse, *Over voltage protection of low voltage systems*, 2nd edition, The Institution of Electrical Engineers, London, United Kingdom, 2000.
3. Ramon de la Rosa, “Contribution to Lightning Research for Transmission Line Compactor”, *IEEE Trans. On Power Delivery*, Vol. 3, No. 2, pp , 1998.
4. Nasrullah Khan, Norman Mariun, Ishak Aris and J Yeak, “Laser-triggered Lightning Discharge”, *New Journal of Physics* 4, August 2002
5. Traeger RK, “The Lightning Arrestor Connector”, *IEEE Trans. On Parts, Hybrid, and Packaging*, Vol. PHP-12, No. 2, pp. 89-94, 1976.
6. M. Brook, C.R. Holmes and C.B. Moore, “Lightning and rockets: Some implication of the Appollo 12 lightning event”, *Naval Research Reviews*, pp. 1-17, 1970.
7. Jean-Claude Diels, “UNM researchers use lasers to guide lightning”, *Campus News*, January 2001.
8. Tutorial, EMC-Zurich, Singapore, 27 February – 3 March 2006.

9. Peter E. Viemeister, *The Lightning Book*, USA: Doubleday & Company, Inc., New York, 1961.
10. Donald W. Zipse, "Lightning Protection System: Advantages and Disadvantages", *IEEE Transaction on Industry Application*, Vol. 30, No. 5, pp. 1351-1361, 1994.
11. Robert Andre, Roubinet Michel, Baumann Jacques, "Lightning Conductor with Piezoelectric Device for Starting the Corona Effect", Patent number: US4728748, 1987.
12. R.J. Van Brunt, Nelson, T.L., Stricklett, K.L., "Early Streamer Emission Lightning Protection Systems: An Overview", *DEIS Feature Article, IEEE Electrical Insulation Magazine*, Vol. 16, No. 1, pp. 5-24, January/February 2000.
13. Z.A. Hartono and I.Robiah, "A Long Term Study on the Performance of Early Streamer Emission Air Terminals in a High Keraunic Region", *Asia-Pacific Conference on Applied Electromagnetic*, pp. 146-150, 2003.
14. Roy B. Carpenter Jr., Mark M. Drabkin, "Protection Against Direct Lightning Strokes by Charge Transfer System", *IEEE Int. Symposium on Electromagnetic Compatibility*, Vol. 2, 1998.
15. Mark M. Drabkin, "Interaction between Lightning Channel and CTS", *IEEE Int. Symposium on Electromagnetic Compatibility*, Vol. 2, pp. 643-647, 1999.
16. Mark M. Drabkin, "Protection Zone of the Charge Transfer System", *IEEE High Voltage Engineering Symposium*, No. 467, pp. 423-425, 1999.

17. Donald W. Zipse, "Lightning Protection Methods: An Update and a Discredited System Vindicated", Industrial and Commercial Power Systems Technical Conference, pp. 155-170, 2000.
18. Donald W. Zipse, "Lightning Protection Methods: An Update and a Discredited System Vindicated", IEEE Transaction on Industry Application, Vol. 37, No. 2, pp. 407-414, 2001.
19. Abdullah M. Mousa, "The Applicability of Lightning Elimination Devices to Substations and Power Lines", IEEE Transactions on Power Delivery, 1998, Vol. 13, No. 4, pp. 1120-1127, 1998.
20. C.B. Moore, William Rison, James Maths, Graydon Aulich, "Lightning Rod Improvement Studies", Journal of Applied Meteorology, Vol. 39, pp. 593-609, 2000.
21. L. M. Ong, H.B Ahmad, N.A. Idris, "The performance of damaged franklin rods", VIII International Symposium on Lightning Protection, 2005.
22. David W. Koopman and T.D. Wilkerson, "Channeling of an Ionizing Streamer by Laser Beam", J. App. Phys, Vol. 42, No. 5, pp. 1883-1886, 1971.
23. Leonard M. Ball, "The Laser Lightning Rod System: Thunderstorm Domestication", J. Applied Optics, Vo. 13, No.10, pp. 2292-2296, October 1974.
24. C.W. Schubert, Jr., and J. R. Lippert, "Investigation into triggering lightning with a pulsed laser", 2nd International Pulsed Power Conference, pp. 132-135. 1979.
25. Megumu Miki, Yoshinori Aihara, Takatoshi Shindo, "Development of Long Gap Discharges Guided by a Pulse CO<sub>2</sub> Laser", J. Phys. D: Appl. Phys, 26, pp. 1244-1252, 1993.

26. Bruno La Fontaine, Francois Vidal, Daniel Comtois, Ching-Yuan Chien, Alain Desparois, Tudor Wyatt Johnston, Jean-Claude Kieffer Hubert P. Mercure, Henri Pepin, Farouk A. M. Rizk, "The influence of Electron Density on the Formation of Streamers in Electrical Discharges Triggered with Ultrashort Laser Pulses", IEEE Trans. On. Plasma Science, Vol. 27, No. 3, June 1999.
27. Takatoshi Shindo, Yoshinori Aihara, Megumu Miki, Toshio Suzuki, "Model Experiment of Laser Triggered Lightning", IEEE Tran. On Power Delivery, Vol. 8, No. 1, pp. 311-317, January 1993.
28. Daniel Comtois, Tudor Wyatt Hohnstion, Jean-Claude Kieffer, Hubert P. Mercure, IEEE Trans. On Plasma Sci, Vo. 28, No. 5, 2002.
29. Megumu Miki, Takashi Shindo, Yoshinori Aihara, "Mechanism of guiding ability of CO2 laser-produced plasmas on pulsed discharges", J. Phys. D: Appl. Phys., pp. 1984-1996, 1996.
30. S. Uchida, Y. Shimada, H. Yasuda, S. Motokoshi, C. Yamanaka, T. Yamanaka, Z. Kawasaki, K. Tsubakimoto, "Laser triggered-lightning in field experiments", J. Opt. Tech., Vol. 66, No. 3, pp. 199-202, 1999.
31. H.B Ahmad, Muhammad Abu Bakar Sidik, and Kwang Ghee Sin, "Method to overcome damage of building structure using laser aided system", in Proceeding Laser and Electro-optics Seminar, Johor, Malaysia, pp. 81-90, June 2006.
32. Z.A. Hartono and I.Robiah, "Location Factor and Its Impact on Antennae Safety with Reference to Direct Lightning Strikes", in Proceeding TENCON, pp. 351-356, 2000.

33. Muhammad Abu Bakar Sidik and Hussein Ahmad, "The review of unconventional Lightning Air Terminal," Institut Voltan dan Arus Tinggi, Internal Report, IVAT/IR/001/2005.
34. Norfizah Binti Othman and Zafirah Binti Abdullah, "Report On The Investigation Of Lightning Related Damages To Buildings Installed With Multipoint-Franklin- Rod," Institut Voltan dan Arus Tinggi, Internal Report, IVAT/IR/002/2005.
35. W. Rison, C.B. Moore, and G.D. Aulich, "Lightning air terminal – Is shape important?," in Proc. International Symposium on EMC, pp. 300 – 3005, August 2004.
36. F.D. Alessandro and G. Berger, "Laboratory studies of corona emissions from air terminals," J. Phys. D: Appl. Phys. 32 pp. 2785-2790, September 1999.
37. K.P. Heary, A.Z. Chaberski, F. Richens, and J.H. Moran, "Early streamer emission enhanced air terminal performance and zone of protection," in Proc. Industrial and Commercial Power Systems Technical Conference, pp. 26-32, 1993.
38. I.D. Chalmers, J.C. Evans, and W.H. Siew, "Considerations for the assessment of early streamer emission lightning protection", IEE Proc. Sci. Meas. Technol. Vol. 146, No. 2, pp. 57-63, March 1999.
39. N.L. Allen, K.J. Cornick, D.C. Faircloth, and C.M. Kouzis, "Tests of the early streamer emission principle for protection against lightning," in Proc. Sci. Meas. Technol, Vol. 145, No. 5, pp. 200-206, September 1998.



40. N.L. Allens, and J.C. Evans, "New investigations of the early streamer emission," in Proc. Sci. Meas. Technol, Vol. 147, No. 5, pp. 243-248, September 2000.
41. M.M. Drabkin, and S. Gryzboski, "Experimental Study of the emission current form ion plasma generator," in Proc. 25th Int. Conf. on Lightning Protection, pp. 385-388, September 2000.
42. Ding Meixin, and Li Huifeng, "Principle and evaluation method of active lightning arrester," in Proc. International Conference on Power System Technology, pp. 1856-1858, 2002.
43. J.B. Lee, S.H. Myung, Y.G. Cho, S.H. Chang, J.S. Kim, and G.S. Kil, "Experimental study on lightning protection performance of air terminals," in Proc. International Conference on Power System Technology, pp. 2222-2226, 2002.
44. L.M. Ong, H. Ahmad, and N.A. Idris, "The Performance of damaged franklin rods," in Proc. VIII International Symposium on Lightning Protection, Sao Paulo, Brazil, pp. , November 2005.
45. H.L. Langhaar. Dimensional Analysis and Theory of Models. New York : John Wiley & Sons, Inc. 1951.
46. J. Alan Chalmers, M.A., Ph.D., F.Inst.P., "Atmospheric Electricity 2nd Edition," Pergamon Press Ltd., 1967.
47. Edward J. Tarbuck, Frederick K. Lutgens, Earth Science 8th Edition, Upper Saddle River, New Jersey 07458, Pearson Education, Inc., 2006.
48. Graham R. Thompson and Jonathan Turk, "Earth Science and the environment, 3rd edition," Brook/Cole, a division of Thomson Learning, Inc., Canada, 2005.

49. Ralph M. Feather Jr., PhD, Susan Leach Snyder, Dinah Zike., "Earth Science," United States of America, Glencoe/McGraw-Hill, 200.
50. Linda Williams, Earth Science Demystified, United State of America, The McGraw-Hill Companies, Inc., 2004.
51. [6] Eric W. Danielson, and Edward J. Denecker, Jr., "Earth Science," Macmillan Publishing Company, a division of Macmillan, Inc., New York, United State of America, 1986.
52. Dale T. Hesser, and Susan S. Leach, "Focus on Earth Science," Merrill Publishing Company, A Bell & Howell Company, United States of America, 1987.
53. Vladimir A. Rakov and Martin A. Uman, "Lightning Physics and Effects," Printed in United Kingdom at the University Press, Cambridge, 2003.
54. Peter E. Viemeister, "The lightning book", MIT Press editon, United State of America, 1972.
55. R.H. Golde, Lightning Protection, Edward Arnold (Publishers) Ltd. 25 Hill Street, London W1X 8LL, Great Britain, 1973.
56. [11] Mark Z. Jacobson, "Fundamental of Atmospheric Modeling," Cambridge University Press, United Kingdom, 2005.
57. M.A. Alam and H. Ahmad, "Review of Lightning Warning Systems: Technical and Economical Aspects," in Proc. Int. Conf. on Electromagnetic Compatibility, Kuala Lumpur, Malaysia, pp. 89-94, April 1995.
58. IEEE Std 1227-1990, "IEEE Guide for the Measurement of DC Electric-Field Strength and Ion Related Quantities".

59. G. Diendorfer, M.Mair, W.Schulz, and W. Hadrian, "Lightning Current Measurements in Austria – Experimental Setup and First Results," in Proc. 25th Int. Conf. on Lightning Protection (ICLP), Rhodos, September 2000.
60. John C. Mosher, Timothy M. Rynne, and Paul S. Lewis, "MUSIC for Localization of Thunderstorm Cells," in Proc. The Twenty-Seventh Asilomar Conference on Signals, Systems and Computers, pp. 986-990, vol.2, Pacific Grove, CA, USA, 1993.
61. Rust W. David, "Initial Balloon Sounding of the Electric Field in Winter Nimbostratus Clouds in the USA," Geophysical Research Letters, Vol. 29, No. 20, pp. 1-4 , 2002.
62. Analog Device, Data Sheet of Integrated Circuit True RMS-to-DC Converter, AD536A.
63. Dearden, A.M.; Harrison, M.D., Impact and the design of the human-machine interface, Aerospace and Electronic Systems Magazine, IEEE, Volume 12, Issue 2, Page(s):19 – 25, Feb. 1997
64. Yamada, T., Human-machine interface for electronic equipment TRON/GUITRON Project International Symposium, The 10th 1-2 Dec. 1993 Page(s):45 – 46, 1993.
65. CJ Liu and DA Wan., Development of a Measuring System Based on LabVIEW for Angular Stiffness of Integrative Flexible Joint, Journal of Physics: Conference Series 48. pp. 521-525. 2006.
66. Wieslaw Winiecki and Michal Karkowski., A New Java-Based Software Environment for Distributed Measuring Systems Design, Ieee Transactions On Instrumentation And Measurement, Vol. 51, No. 6, Pp. 1340-1346, December 2002.

67. Orobchuk, B., Increasing of the self-descriptiveness of the research and diagnostics of an allergy to medicines through the usage of a computer measuring system CAD Systems in Microelectronics, CADSM 2003. Proceedings of the 7th International Conference. The Experience of Designing and Application of, 18-22 Feb. 2003 Page(s):159 – 160, 2003.
68. Douglass C. Montgomery, George C. Runger, and Norman Faris Hubele., Engineering Statistic 2nd Edition, John Wiley and Sons, Inc., New York. 2001.
69. Chung-Ping Young; Devaney, M.J.; Shyh-Chyang Wang; Universal serial bus enhances virtual instrument-based distributed power monitoring, Instrumentation and Measurement, IEEE Transactions on Volume 50, Issue 6, Page(s):1692 – 1697, Dec. 2001.
70. Ramamurthy, G.; Ashenayi, K.; Comparative study of the FireWire/spl trade/ IEEE-1394 protocol with the Universal Serial Bus and Ethernet Circuits and Systems, 45<sup>th</sup> Midwest Symposium on Volume 2, 4-7 Page(s):II-509 - II-512 vol.2, Aug. 2002.
71. S Tumanski, Principle of Electrical Measurement, Taylor & Francis, New York, 2006.
72. Md. Ahsanul Alam, The Study of Lightning Ground Flash Phenomena in Peninsular Malaysia, Master Thesis, Universiti Teknologi Malaysia, 1996.
73. Geology and Earth Science, <http://geology.com/world/malaysia-satellite-image.shtml> , access on May 2007.
74. Geology News – Earth Science Current Events, Wednesday, December 14, 2005, [http://geology.com/news/2005/12/lightning-map\\_14.html](http://geology.com/news/2005/12/lightning-map_14.html) , access on May 2007.

75. Jabatan Meteorology Malaysia (JMM), <http://www.kjc.gov.my/> , access on May 2007.
76. Charles Green, “Electrostatics Hand Book”, Hawan Sams Publication, 1973.